Managing Solar Uncertainty in Neighboring Systems

With Stochastic Unit Commitment

by

Robin Broder Hytowitz

A Thesis Submitted in Partial Fulfillment
of the Requirements for the Degree
Master of Science

Approved July 2013 by the
Graduate Supervisory Committee:

Kory W. Hedman, Chair
Gerald T. Heydt
Raja Ayyanar

ARIZONA STATE UNIVERSITY

August 2013

ABSTRACT

As renewable energy becomes more prevalent in transmission and distribution systems, it is vital to understand the uncertainty and variability that accompany these resources. Microgrids have the potential to mitigate the effects of resource uncertainty. With the ability to exist in either an islanded mode or maintain connections with the main-grid, a microgrid can increase reliability, defer T&D infrastructure and effectively utilize demand response. This study presents a co-optimization framework for a microgrid with solar photovoltaic generation, emergency generation, and transmission switching. Today unit commitment models ensure reliability with deterministic criteria, which are either insufficient to ensure reliability or can degrade economic efficiency for a microgrid that uses a large penetration of variable renewable resources. A stochastic mixed integer linear program for day-ahead unit commitment is proposed to account for uncertainty inherent in PV generation. The model incorporates the ability to trade energy and ancillary services with the main-grid, including the designation of firm and non-firm imports, which captures the ability to allow for reserve sharing between the two systems. In order to manage the computational complexities, a Benders' decomposition approach is utilized. The commitment schedule was validated with solar scenario analysis, i.e., Monte-Carlo simulations are conducted to test the proposed dispatch solution. For this test case, there were few deviations to power imports, 0.007% of solar was curtailed, no load shedding occurred in the main-grid, and 1.70% load shedding occurred in the microgrid.

To my husband,

your encouragement supported me through this great endeavor

and will continue to support me in the many adventures to come.

ACKNOWLEDGEMENTS

I would like to thank my adviser, Professor Kory Hedman, for his guidance on my research. He has encouraged me from the beginning of my graduate career to take challenging courses, think critically and carefully, and strive to make my work better. I appreciate his patience and dedication to helping his students. I discovered my passion for power systems engineering with his help and could not be more grateful for his advice and support.

I would also like to thank my two committee members, Professor Gerald Heydt and Professor Raja Ayyanar. I appreciate your feedback and assistance with my thesis. I am also grateful to the entire Electric Power and Energy Systems faculty. I have learned so much in the last two years and I am thankful to study with so many knowledgeable professors. To my friends and classmates, I thank you for helping and motivating me along the way. I would also like to thank my parents, they have always been a strong support for my academic endeavors.

Finally, I am grateful to ASU LightWorks for providing funding for this project under the TerraWatt Challenge. I would especially like to thank Professor Stephen Goodnick, who taught me basic circuitry and introduced me to this project.

TABLE OF CONTENTS

LIST OF TABLES

Table Page

LIST OF FIGURES

Figure Page

I. NOMENCLATURE

The letter on the far right indicates if the symbol represents a parameter (P), set (S), or variable (V). The symbols are listed in alphabetical order by Latin characters followed by Greek characters.

B_k	Line susceptance for line k	P
b_z	The right hand side of the constraints in the subproblem for constraint z	P
BUS	Nodes in the system	S
C_T	Maximum number of open lines connecting the main- and microgrid in hour T	P
c_g	Linear cost of generator g	P
c_T^{+F}	Cost to sell firm imports to the main-grid in hour T	P
c_T^{-F}	Cost to buy firm imports from the main-grid in hour T	P
c_T^{+NF}	Cost to sell non-firm imports to the main-grid in hour T	P
c_T^{-NF}	Cost to buy non-firm imports from the main-grid in hour T	P
c_g^{NL}	No load cost of generator g	P
c_g^{SU}	Start up cost of generator g	P
c_g^{SD}	Shut down cost of generator g	P
$d_{i,t}$	Demand in microgrid at bus i for period t	P
E_T^+	Indicator that power is being sold (1) in hour T	V
E_T^-	Indicator that power is being purchased (1) in hour T	V
$g(i)$	Set of generators at bus i	P
GEN	All generators in the system	S
$HOUR$	Hours in a day	S
$LINE$	Lines connecting all buses in the system	S
M_k	Big M value for intertie line k	P

M^{ζ}	Big M value for total cost of main-grid	P
$MAIN$	Generators in the main-grid	S
$MICRO$	Generators in the microgrid	S
MIN	Five-minute periods in a day (288)	S
$P_{g,t,c}$	Power output from generator *g* in period *t* for contingency *c*	V
$\overline{P_{g,T}^{MAIN}}$	Total power in the main-grid fixed in stage one	P
P_g^{max}	Maximum power capacity for generator *g*	P
P_g^{min}	Minimum power capacity for generator *g*	P
$P_{k,t,c}$	Power flowing in line *k* in period *t* for contingency *c*	V
P_k^{max}	Maximum line rating for line *k*	P
P_k^{min}	Minimum line rating for line *k*	P
P_t^{+F}	Net firm power sold to the main-grid in period *t*	V
P_t^{-F}	Net firm power purchased from the main-grid in period *t*	V
P_t^{+NF}	Net non-firm power sold to the main-grid in period *t*	V
P_t^{-NF}	Net non-firm power purchased from the main-grid in period *t*	V
P_T^{+F}	Average net firm power sold to the main-grid for hour *T*	V
P_T^{-F}	Average net firm power purchased from the main-grid for hour *T*	V
P_T^{+NF}	Average net non-firm power sold to the main-grid for hour *T*	V
P_T^{-NF}	Average net non-firm power purchased from the main-grid for hour *T*	V
$P_{g,t,c}^{NSP}$	Additional power reserve in the stage three for generator *g* in period *t* for contingency *c*	V
$P_{i,t,c}^{PV}$	Power from solar PV at bus *i* in period *t* for contingency *c*	P
$P_{i,t,c}^{PVcurtail}$	Solar power curtailed at bus *i* in period *t* for contingency *c*	V
R_g	Hourly generator ramp rate for generator *g*	P
R_g^5	Five-minute ramp rate for generator *g*	P
R_g^{SU}	Ramp up rate for generator *g*	P
R_g^{SD}	Ramp down rate for generator *g*	P

$r_{g,T}^{SP}$	Spinning reserves from generator *g* in hour *T*	V
$r_{g,T,c}^{NSP}$	Non-spinning reserves from generator *g* in hour *T*	V
$S_{i,t}$	Load shedding in stage three to ensure feasibility for bus *i* in period *t*	V
$SCEN$	Contingencies in the stochastic linear program	S
$u_{g,T}$	Commitment of generator *g* in hour *T*	V
$u_{g,T,c}^{NSP}$	Variable indicating if the non-spinning generators are on (1) or off (0) in stage two for generator *g* in period *T* for contingency *c*	V
$\overline{u_{g,t,c}^{NSP}}$	Fixed commitment status for non-spinning generators that are on (1) or off (0) in stage two for generator *g* in period *t* for contingency *c*	P
$v_{g,T}$	Start up commitment of generator *g* in hour *T*	V
$w_{g,T}$	Shut down commitment of generator *g* in hour *T*	V
Z	Constraints in the subproblem (stage three)	S
$z_{k,T}$	Variable indicating if intertie line *k* is closed (1) or open (0) in hour *T*	V
$\delta^{+}(i)$	Set of lines defined as connected to bus *i*	P
$\delta^{-}(i)$	Set of lines defined as connected from bus *i*	P
Δ_t^{+F}	Deviation from averaged firm power sold to the main-grid in period *t*	V
Δ_t^{-F}	Deviation from averaged firm power purchased from the main-grid in period *t*	V
Δ_t^{+NF}	Deviation from averaged non-firm power sold to the main-grid in period *t*	V
Δ_t^{-NF}	Deviation from averaged non-firm power purchased from the main-grid in period *t*	V
ζ_T	Binary variable ensuring the Pareto constraint is not violated in hour *T*	V
η	The objective of the master problem (stage two)	V
$\theta_{k,t,c}$	Voltage angle of the line *k* in period *t* for contingency *c*	V
θ^{max}	Maximum angle rating	P
θ^{min}	Minimum angle rating	P
κ_t^{+F}	Penalty for deviating from average firm imports sold to the main-grid in period *t*	P

κ_t^{-F}	Penalty for deviating from average firm imports purchased from the main-grid in period *t*	P
κ_t^{+NF}	Penalty for deviating from average non-firm imports sold to the main-grid in period *t*	P
κ_t^{-NF}	Penalty for deviating from average non-firm imports purchased from the main-grid in period *t*	P
λ_z^y	The dual variables of constraints from the subproblem for iteration *y* and constraint *z*	V
ρ_c	Probability that scenario *c* will occur	P
τ_g^{UT}	Minimum generator up time	P
τ_g^{DT}	Minimum generator down time	P

II. INTRODUCTION

With the increase in renewable energy resources, reliability and uncertainty have become essential issues facing system operators and planners. Solar photovoltaic (PV) generation is subject to a great deal of variability and uncertainty, depending on the size and location of the array. The issues caused by PV arise from weather events, such as rain and dust storms, cloud cover, and inaccurate solar forecasts. PV arrays in remote areas, or those without any kind of storage, might necessitate curtailment in some electric grids. Battery systems pair well with renewable energy, but are often cost prohibitive; small microgrids might not be able to afford enough energy storage to truly lessen the effects of solar variability. Microgrid systems are one resource that can help mitigate the effects of solar. In addition to its ability to operate in an islanded mode, the control and management of a microgrid can be more sophisticated and complex than a larger, traditional grid system. The intricacy by which power generation and main-grid interactions are modeled can increase due to the small-scale topology of a microgrid.

Microgrid systems have the ability to depend on their neighboring electric grids since operating two grids together will further improve reliability and reduce costs. There are presently neighboring systems that trade power and depend on each other for ancillary services. The system described in this paper attempts to mimic the regional relationship between entities, as opposed to a small residential neighborhood and its system operator. For example, this neighboring system could compare to an entity, such as the Sacramento Municipal Utility District (SMUD), who might trade with a larger entity, e.g., the California Independent System Operator (CAISO). For simplicity, we refer to the smaller neighboring system in the model as a microgrid, though the work

developed in this paper can be used by any single entity that is integrated into a larger network.

The modeling of the microgrid in this paper involves many complexities, e.g., a stochastic mixed integer program, which are typically not used within a large-scale system. However, advances in stochastic programming are being developed. Decomposition techniques like progressive hedging might soon be able to quickly handle problems of this magnitude, [1].

There are political and social factors that justify the use of microgrids to mitigate uncertainty. Military bases cannot always depend on the surrounding area for uninterrupted electricity support. In these cases, a microgrid with islanding capabilities can ensure that power remains online even if the surrounding area faces a blackout. Microgrids can also benefit communities that choose to promote solar energy, allowing them greater control over their power generation mix. A microgrid with PV will greatly increase its ability to provide reliable electricity, with the addition of emergency generators and/or storage.

In order to manage PV uncertainty, this research presents a stochastic mixed integer program, which is decomposed into three stages to reduce the computational burden. The model also incorporates a complex relationship between two interconnected systems that can trade and switch the intertie lines between them. The model is intended to capture existing flexibility between systems while also ensuring scalability for larger electric grids with advances in stochastic programming algorithms.

The contributions of this work are:

- A modeling framework describes the complex interactions between two neighboring electric grids while ensuring Pareto improvements for each system. The model includes the trade of ancillary services and energy (firm and non-firm imports) in order to improve the efficiency of both systems and provide each system the opportunity to anticipate the operating conditions of the other.
- A multi-stage stochastic programming problem for day-ahead scheduling, which incorporates solar uncertainty at the 5-minute level. Unlike previous work, the 5-minute interval expresses detailed variability about solar generation in a day-ahead framework, instead of using hourly averages that do not capture the imposed ramping requirements of solar power.
- A transmission switching model to allow the neighboring system to decide to disconnect intertie lines in order to minimize loop flow and wheeling through its system.
- Solar scenario analysis is conducted to confirm the approach. Many stochastic models do not validate their solution against a wide array of scenarios. The results from this research were validated against Monte Carlo simulations to establish with confidence the effectiveness of the model.

This research is organized into the nine following chapters. Chapter I describes the nomenclature used in the research. The topic is introduced in Chapter II, followed by a review of the current research on the topic in Chapter III. The basics of power flow modeling will be described in Chapter IV with a focus on optimal power flow and unit

commitment. A description of the types of uncertainty modeling and the methodology utilized for this research are in Chapter V. The problem is described Chapter VI, specifying the motivation behind each of the three stages and their mathematical formulation. Chapter VII gives the results of the simulations. Chapter VIII discusses the conclusions of this research and future work. The references are included at the end of the thesis. The code created for this model can be made available upon request to the author.

III. Literature Review

The literature covered in this chapter will focus on several key aspects of the research project. First, uncertainty modeling in power systems will be examined through different types of mathematical programs. Next, research on variability due to renewable energy will be discussed. Finally, literature concerning microgrids will be covered. Similar to the concept of a microgrid used in this research, the literature focuses on small systems that are completely or semi-autonomous from a larger system. Since the system used here does not fall into most specific definitions of a microgrid, official or formal definitions will not be addressed.

Uncertainty is a feature in many aspects of the electric grid and in power systems engineering. There are several traditional sources of uncertainty, especially in power flow and unit commitment (UC) problems. These problem formulations typically include a value for load, which is susceptible to large forecast errors. Without improvements in the forecast, these uncertainties can persist over time and cause inefficient solutions. In addition to load, unreliable equipment can cause faults and outages adding uncertainty to a system. Recently, renewable energy has added generation uncertainty to the electric grid. Many researchers have considered how this new source of generation will impact the grid; there is still much that is unknown and much to be perfected. Due to the traditional sources as well as the increase of renewable energy in the grid, uncertainty modeling is a topic of interest in power systems literature.

General optimization methods for dealing with uncertainty in various problems and industries are reviewed in [2]. Sahinidis does not specifically focus on power systems, but offers an overview of many types of modeling that deal with uncertainty:

stochastic programming, fuzzy programming, stochastic dynamic programming, and probabilistic programming among others. Some of these methods have been well researched for power systems applications, specifically robust programming, fuzzy programming, and stochastic programming. The following review will cover several types of uncertainty modeling, while the theory will be covered in the next chapter.

Although the literature is not as extensive as stochastic or robust programming, some research has been done on fuzzy programming in power systems. Optimal power flow is performed in [3] and [4], the Peruvian system is tested in a fuzzy power flow in [5], and a study of UC was done in [6] where load, incremental cost, start-up cost, and production cost were the uncertainties. One fuzzy UC methodology specifically integrates solar power, and mitigates some of the variability by modeling a battery system in [7].

Robust optimization is a widespread method researchers use to study uncertainty in power systems. Many have used the programming method to study UC and generation scheduling problems. In [8], a generation schedule is created by testing extreme wind scenarios in a robust optimization framework, which they call robust scheduling. They use error terms and a penalty function to identify solutions that might be infeasible in a stochastic model, but are present in their robust scheduling model. Finitely adaptable robust linear programming is used to calculate day-ahead locational marginal prices for a small and medium system in [9].

The following papers focus on robust UC problems with a similar framework as the model used in this research. While this research focuses on solar power, it is helpful to compare methodologies from demand, generation, and wind uncertainty. A two-stage

robust integer programming model in [10] examines generation and demand uncertainty for cases with and without transmission limits and ramp rates. They show that their UC model can provide a more cost effective solution compared to the worst-case scenario. A three stage robust program is developed in [11] that considers wind and demand response uncertainty. In the first stage, UC is done with both factors as unknowns. The second and third stages maximize social welfare for worst-case scenarios of wind and price-elastic demand respectively. Due to the complexity of the model, Benders' decomposition was used for the IEEE 118-bus test case. Their results show that the solutions only considering wind uncertainty were higher in cost than those only considering demand response uncertainty. A two-stage adaptive robust optimization approach is used to solve a security constrained UC problem in [12]. They use a decomposition method that combines Benders' decomposition and an outer approximation method for the second stage. The model is tested against the ISO New England system for reliability and efficiency. Robust optimization was also used in a two-stage minimax regret technique for the UC problem under wind uncertainty in [13].

While less information is needed about the uncertainties in a robust program, this method can often provide an overly conservative result. With a large system, a conservative result can often be a desired tradeoff compared with the computational burden of other methodologies, like stochastic programming. Some researchers have attempted to combine these approaches. A unified stochastic robust approach was proposed in [14]. With the use of Benders' decomposition, they created a framework that is less conservative compared to a traditional robust optimization model.

Stochastic programming focuses on a probabilistic uncertainty set, which complements the types of uncertainties in many power systems problems. The stochastic problem dealing with uncertainty in power demand and generation outages was formulated in [15] using scenario trees and in [16] using a variety of produced scenarios. Demand uncertainty and random outages were also modeled in [17] using Lagrangian relaxation to decompose a security-constrained UC problem. They recommend utilizing a scenario reduction strategy due to the large computational burden of stochastic programming. The combination of stochastic unit commitment and reserve requirements was analyzed in [18], where the resulting schedules were found to be more robust.

These techniques have also been applied to uncertainty in renewable energy generation, especially wind uncertainty. Particle swarm optimization was used to solve a stochastic UC considering wind generation uncertainty in [19]. Scenario reduction techniques were used to create a scenario set that is more computationally tractable from 23 branching stages of a multi-stage scenario tree. The authors in [20] study the impact of wind uncertainty on unit commitment using rolling planning with scenario trees, and they find a reduction in costs compared to deterministic modeling. Reference [21] considers wind uncertainty in four types of electricity markets and one heat market. The stochastic model is a multi-stage recursion model; this is possible because new information about a grid system becomes available in waves, which allows recourse decisions to be made after some of the uncertainties have been established. Many papers have been published that specifically deal with various aspects of wind generation uncertainty in UC: reserve and security [22], impacts on thermal units [23], security-constrained considering volatility [24], using interval linear programming [25], and chance-constrained [26].

Compared to solar, wind uncertainty has been fairly well researched, especially for the UC problem.

Some research has combined solar uncertainty with other forms of uncertainty in large problems. The California system was examined in [27] using stochastic wind and solar forecast errors from actual historical data and a statistical model described in [28]. In [29], they use particle swarm optimization to demonstrate cost and emissions reduction when modeling grid-tied vehicles, renewable resources, and demand side uncertainty.

Solar specific uncertainties and methods have not been as well studied as load or wind uncertainty. Most of the solar research is focused on the changing nature, or variability, of solar rather than the unknown properties, or uncertainty. Early studies simply integrated solar as a deterministic resource to schedule units [30]. More recent models use different statistical methods to predict solar radiation, like autoregressive moving average (ARMA) [31] or artificial neural networks (ANN) [32]. A mathematical and neural network prediction model is used for radiation data in Singapore in [33]. In [34] an adaptive nonlinear autoregressive exogenous model (NARX) network is used to predict solar PV output with little information from historical data by using Hottel's radiation model under clear sky conditions. Particle swarm optimization is used in [35] to solve UC with wind, solar, and battery resources; however, they assume the wind and solar forecasts are accurate, meaning there is no consideration of uncertainty. The variability of longer time horizons was examined in [36], with additional attention paid to larger spatial areas. Different statistical models are explored in [37], each dealing with the unique characteristics of load, wind and solar. Overall, few if any research has truly combined the uncertainty and variability of solar power generation. The formulation in

Chapter VI hopes to identify the components of each and incorporate them into the model.

In addition to solar modeling, this research is focused on creating a model framework for a microgrid system. Microgrids can be generally described as small systems that have the ability to control their resources and operate autonomously. The basic power issues for microgrids are described in [38] and a general review of microgrid technology is found in [39], which focuses on the ability of a microgrid to control disturbed renewable energy resources.

In 2001, [40] defined a small cluster of loads and generation sources that could exist somewhat autonomously as a microgrid, emphasizing the flexibility and control that accompanies smaller systems, while still allowing economic trade between them. The author also introduces one of the more well-established microgrid development sites – the Consortium for Electric Reliability Technology Solutions (CERTS) at Lawrence Berkeley National Lab.

In describing microgrids as they relate to the future of the electric grid, [41] describes three potential benefits: combined heat and power, power quality and reliability, and the role of the decision maker. A small community is a natural heat sink and would allow onsite generation to transport excess heat without unnecessary transportation loss. The authors also suggest that power quality and reliability need not be universal and can follow a pyramid structure comparing requirement and necessity; certain loads can be designated for lower quality and/or reliability than others and, consequently, pay a lower cost. Finally, the decision maker in a microgrid wields more

purchasing power than an operator in a main-grid and, thus, the decision maker can decide to implement certain technologies over others.

Much of the literature on the role microgrids play in the future claims they are essential for advances to the smart grid, noting their islanding capabilities and enhanced control as especially relevant. In [42], they focus on a microgrid's ability to island and necessary conditions for reconnecting to the main-grid. They also describe how microgrids can act as cost saving measures, such as the conversion of a small old distribution system to microgrid without necessitating large changes to the entire network. Looking at microgrids from a system-wide perspective, [43] suggests that the future smart grid will be composed of a series of microgrids. The microgrids allow customers to take more active roles in their electricity consumption and allows operators to run small simulations before implementing on a large scale. They use a Fully Connected Neuron network to simulate an energy management system on a 23-bus system. Both of these concepts of a microgrid are similar to the system described in this research: microgrids can be highly flexible and encourage operators to decide how the system should be managed.

Many have distinguished power flow modeling for a microgrid due to its ability to island itself from the main-grid and the significant impact of renewables. A discussion of possible reserve requirements for economic dispatch is found in [44]. Microgrid control and operation with high penetration of distributed generation and renewable energy is researched in [45]. In order to better handle local control and rely less on centralized dispatch, they recommend the use of small scale microgrids. Many have also examined different modeling techniques for a microgrid in a UC framework: renewables with

dynamic programming [46], optimizing both CO_2 emissions and fuel prices [47], renewables in grid-connected versus islanded mode [48], renewables using a genetic algorithm [49], integrating emissions costs, battery storage, fuel cells, and renewables [50], high reliability distribution system switches [51], using a rolling horizon strategy [52], and prioritizing the minimization of customer payment before maximizing reliability [53].

There is a great deal of literature dealing with renewable energy and microgrids and the types of mathematical programming that can help address uncertainty in those systems. Most research on uncertainty and variability in renewable energy has focused on wind power, analyzing the different programming techniques and optimization approaches used to deal with uncertainties. When these authors consider solar, they often overlook either uncertainty or variability, clumping solar into a general renewable energy category. Renewables have been analyzed in the context of a microgrid, both within the UC framework and for other types of problems. Many have pointed to microgrids as building blocks for the future electric grid due to their controllability and reliability. Few, if any, have created detailed models of a microgrid's interactions with its neighbor to take advantage of that controllability in order to temper the effects of renewable energy. The model described in Chapter VI demonstrates how a small system can leverage its relationship with its neighbors to create a reliable and cost efficient system with a high penetration of solar energy.

IV. Power Flow Modeling

Representations of power flow models are essential for engineers operating the electric grid and planning for future expansions. There are both basic ways to represent power flowing through a network, and highly complex methods with a cumbersome computational burden. The following sections discuss the two methods used in this research, as well as a description of their assumptions.

A. Optimal Power Flow

The term optimal power flow (OPF) can take on different meanings depending on the context and problem described. First, the basic theory behind power flow will be discussed, followed by the different types of power flow and optimal power flow models. Finally, the specific use of the direct current optimal power flow will be explained.

The general term *power flow* or power flow study refers to a set of equations that describes the flow of electrons in a networked system. There are several components that are often found in power flow studies: a network topology, line impedances/admittance values, load (active and reactive), generation resources (including a slack bus), and expected voltages. Typically, transmission lines are represented by a pi-equivalent circuit. A set of equations composed of these constituent parts can then be developed and solved. The equations can be non-linear if reactive power is included and voltage is not assumed to be approximately one per unit. These non-linear equations can be difficult to solve, especially as the number of buses grows. For a more detailed description of the problem and methods to solve simultaneous nonlinear equations, see Chapter 4 in [54].

In addition to a basic power flow, operators and planners are often interested in the costs of a system. Economic dispatch is one method to determine the optimal mix of

generation to meet a particular load. Economic dispatch does not usually include network constraints, but does include generator capacity limits. A single bus, generators, and a cumulative load will typically represent the network. In both of these cases, the load is considered inelastic, meaning that it has a vertical demand curve.

Optimal power flow (OPF) contains aspects from economic dispatch and power flow problem. Generally, OPF problems consider the cost of the system in its objective and include the equations that make up a power flow problem as constraints. These constraints limit generator production, transmission line flow, voltage limits, as well as others depending on the amount of detail required in the problem. To consider the problem in its entirely, without many assumptions, it becomes a non-linear problem called an alternating current OPF (ACOPF). In addition to limits on power production and a node balance equation, an ACOPF is defined by the following power balance equations, which define the real (4.1) and reactive (4.2) power transferred on line *k* from bus *m* to bus *n*.

$$P_k^{nm} = V_m^2 G_k + V_m^2 G_m - V_n V_m (G_k \cos(\theta_m - \theta_n) + B_k \sin(\theta_m - \theta_n)) \quad (4.1)$$

$$Q_k^{nm} = -\left(V_m^2 B_k + V_m^2 B_m + V_m V_n (G_k \sin(\theta_m - \theta_n) - B_k \cos(\theta_m - \theta_n))\right) \quad (4.2)$$

V_n and V_m are the voltage magnitudes at bus *n* and *m* respectively, and θ_n and θ_m are the voltage angles at bus *n* and *m* respectively. G_k is the series conductance and B_k is the series susceptance of line *k*. G_m is the shunt conductance and B_m is the shunt susceptance of the line at bus *m*.

These equations, along with their counterparts describing the flow from bus *n* to bus *m*, compose the equality constraints in the ACOPF. They create the solution space, which is optimized to produce a solution with the least cost generation. The objective of

the ACOPF is minimizing the cost of generation; however, some choose to minimize the losses in the system. Some OPF formulations also include contingency analysis, which adds constraints based on the loss of a single component of the system (generators, transmission lines).

J. Carpentier first introduced the ACOPF in 1962 in the French journal *Bulletin de la Société Française des Électriciens*. Since then it has been well studied; however, it is still not easily solved due to the non-linearities. There are many ways to solve an OPF, including the Gauss-Seidel method, the Newton-Raphson method, steepest descent method, conjugate gradient method, and non-linear optimization. A discussion of these methods applied to power systems can be found in Chapter 4 of [54] or in [55]. A comprehensive discussion of the history, formulation, solution techniques and some computational testing for the ACOPF can be found in [55], [56], [57], [58].

The ACOPF is a difficult problem to solve. While advances in computational power are growing, there are alternative ways to gain similar results with less computational burden. The direct current OPF (DCOPF) is one such way. The name is a misnomer, since the method does not involve dc power; rather it is a linearization of the ACOPF. The DCOPF makes four general assumptions in order to linearize an otherwise nonlinear set of equations. First, it is assumed that the voltage magnitudes are close to one per unit. This assumption might not necessarily be true for the distribution system, but is reasonable for the transmission system.

The second assumption is the resistance of the transmission line is very small, much smaller than the impedance of the line. In the power flow equation, the susceptance B_k is defined as $\frac{-X_k}{R_k^2+X_k^2}$, and with $R_k \ll X_k$, can be reduced to $\frac{-1}{X_k}$. Because the resistance is

so small, the DCOPF is considered a lossless model. Unlike the ACOPF, the power on line *k* from bus *n* to bus *m* is equal to the flow from bus *m* to bus *n*. Additionally, the shunt conductance is very small and, therefore, negligible. Third, it is assumed that the voltage angle difference on the line between the buses is small. This means that $\sin(\theta_m - \theta_n) \approx \theta_m - \theta_n$ and $\cos(\theta_m - \theta_n) \approx 1$. Finally, reactive power is ignored. These assumptions transform (4.1) as follows:

$$P_k^{nm} = G_k - G_k - B_k(\theta_m - \theta_n) = B_k(\theta_n - \theta_m) \tag{4.3}$$

In addition to the power flow equality constraint, the DCOPF also contains the same generator and transmission line constraints of the ACOPF, found (4.5)-(4.9). The objective of the DCOPF is typically to minimize the costs of generating power (4.4). This basic formulation is a linear program and therefore easier to solve than the ACOPF. It is also the basis for unit commitment, which will be described in the next section.

DCOPF Formulation:

$$\min \sum_{\forall g} c_g P_g \tag{4.4}$$

Subject to

$$P_g^{min} \leq P_g \leq P_g^{max}, \ \forall\, g \tag{4.5}$$

$$P_k^{min} \leq P_k \leq P_k^{max}, \ \forall\, k \tag{4.6}$$

$$\theta^{min} \leq \theta_n - \theta_m \leq \theta^{max}, \ \forall\, k \tag{4.7}$$

$$P_k = B_k(\theta_n - \theta_m), \ \forall\, k \tag{4.8}$$

$$\sum_{\forall k \in \delta^+(i)} P_k - \sum_{\forall k \in \delta^-(i)} P_k + \sum_{\forall g \in g(i)} P_g = d_i, \forall i \tag{4.9}$$

B. Unit Commitment

The previous section discusses different power flow formulations, including the optimal power flow. OPFs solve a network for optimal generation cost with assumptions about the state of the generators in the system. These assumptions cannot be made for power flow problems run day-ahead, when generation schedules are not finalized. In order to optimize the state and status of generators in a network for the next day, the unit commitment formulation must be utilized. As the name states, it will generate (at minimum) the commitment schedule of the generators (units) in the network. The objective and constraints of the unit commitment (UC) formulation aim to operate the network reliably and at least cost.

All of the constraints included in the OPF described previously are included in the UC formulation with some adjustments. In order to determine the statuses of the generators, a binary variable must be introduced to the problem, $u_{g,T}$. Typically, a value of 1 represents an "on" status and 0 an "off" status. This variable makes the problem a mixed integer linear program (MILP), which is difficult to solve. This new variable is incorporated into the upper and lower bounds of the generator capacity constraint, (4.11), which will force the power generation variable, $P_{g,T}$, to 0 if the generator is off.

UC formulations will often include startup and shutdown variables in addition to the commitment status variables. These variables will also take values of either 0 or 1 if the generator is starting up or shutting down within the period; however, they do not necessarily need to be integer (binary) variables. The constraints can be written in such a way that forces the variable to take on a value of either 0 or 1. The constraints, including the upper and lower bounds, can be found in (4.15)-(4.17). The startup variable will be

one in the first period that the commitment variable is one, and the shutdown variable will be one the first period the commitment variable is zero. In addition to the variables, there is a cost associated with starting up and shutting down. These two fixed costs are added to the objective function, (4.10), along with the linear cost function for the power dispatched.

Thermal generators have optimal operating points. Constantly turning generators on and off will cause them to deteriorate faster and require more maintenance. Because of this, minimum up and down times are added to the UC formulation. These constraints dictate the amount of time a generator must be on before it can be turned off again, meaning a generator must stay on *x* number of hours before shutting down. This constraint, among others, makes the UC problem an inter-temporal problem. Unlike the OPF, which can be solved for individual periods separately, the UC problem is solved for all periods in order to find the optimal schedule for the generators given their temporal constraints. There are several ways to write the constraints and produce the same solution; however, (4.20) and (4.21) ease the computational burden of the problem. A proof and analysis can be seen in [59].

Power dispatched is limited by the generator ramp rate. Generators have specified ramp rates for periods when they startup, shutdown, and in between hours or periods in the UC formulation. These four ramp rates can be succinctly written in two inter-temporal constraints (4.18)-(4.19) using the commitment variable $u_{g,t}$. An analysis of the ramp rate constraints can be found in 3.5.6 of [60].

Several reviews have been published on UC in 1994 [61], and 2004 [62], [63]. These can be referenced for further information on additional constraints, formulations,

and solution methodology. In this paper, mixed integer programming is used to solve the UC model in Stage Two described in Chapter VI-C-2.

Unit Commitment Formulation

$$\min \sum_{\forall T} \sum_{\forall g} \left(c_g P_{g,T} + c_g^{SU} v_{g,T} + c_g^{NL} u_{g,T} \right) \tag{4.10}$$

Subject to

$$u_{g,T} P_g^{min} \leq P_{g,T} \leq u_{g,T} P_g^{max}, \ \forall \ g, T \tag{4.11}$$

$$P_k^{min} \leq P_{k,T} \leq P_k^{max}, \ \forall \ k, T \tag{4.12}$$

$$\theta^{min} \leq \theta_{n,T} - \theta_{m,T} \leq \theta^{max}, \ \forall \ k, T \tag{4.13}$$

$$P_{k,T} = B_k \left(\theta_{n,T} - \theta_{m,T} \right), \ \forall \ k, T \tag{4.14}$$

$$v_{g,T} - w_{g,T} = u_{g,T} - u_{g,T-1}, \ \forall \ g, T \tag{4.15}$$

$$0 \leq v_{g,T} \leq 1, \ \forall \ g, T \tag{4.16}$$

$$0 \leq w_{g,T} \leq 1, \ \forall \ g, T \tag{4.17}$$

$$P_{g,T} - P_{g,T-1} \leq R_g u_{g,T-1} + R_g^{SU} (v_{g,T}), \ \forall \ g, T \tag{4.18}$$

$$P_{g,T-1} - P_{g,T} \leq R_g u_{g,T} + R_g^{SD} (w_{g,T}), \ \forall \ g, T \tag{4.19}$$

$$\sum_{r=T-\tau_g^{UT}+1}^{T} v_{g,r} \leq u_{g,T}, \ \forall \ g, T \tag{4.20}$$

$$\sum_{r=T-\tau_g^{DT}+1}^{T} w_{g,r} \leq 1 - u_{g,T}, \ \forall \ g, T \tag{4.21}$$

V. UNCERTAINTY MODELING

The variables and parameters in power flow and unit commitment models discussed in Chapter IV are assumed to be deterministic, meaning their parameters and variables have one set of values that will not change. With ample knowledge of a power system, this assumption might suffice. However, many factors in a power system are not known or certain. Generator outages, transmission line outages (permanent faults), deviations to import schedules, and load forecast error are among the traditional uncertainties in electric power systems. Many have considered the impacts of load forecast error; customer demand changes in different ways from minute to minute, day to day, and year to year. While there might be a methodological forecast for the increase demand over time, there is still no absolute certainty for how demand will behave in real time. Therefore, it is essential to consider the impact of uncertainty on the power system. There are several methods used to manage uncertainty, many of which will be discussed in the first section. The discussion will culminate in stochastic programming, which was used to solve the model described in Chapter VI. The method used to generate the stochastic scenarios will be covered in Part B of this chapter.

A. Types of Uncertainty Modeling

One of the most basic ways to handle uncertainty is sensitivity analysis. This type of analysis evaluates a solution from a problem that did not integrate uncertainty into the formulation and it tries to find a tolerance for the given solution. While it attempts to consider uncertainty, the solution was not gained from a problem that optimized under uncertain terms. Due to the significant uncertainty related to renewable energy, sensitivity analysis will not suffice. Instead, programming techniques that deal with

uncertainty will be evaluated for their applicability to solar generation and to power systems problems.

1) Reserve Requirements

Historically, reserve requirements can be implemented as constraints in the unit commitment problem to account for uncertainty due to damaged equipment or forecast error. Small fluctuations in power are not covered by reserve requirements. Regulatory standards cover fluctuations that occur on a second-by-second time scale with the use of automatic generation control (AGC). AGC is responsible for maintaining frequency at 60 Hz and managing unforeseen changes in power, such as the flow between balancing areas. While small variations in solar output might be covered by AGC, a sudden drop to 30% of peak capacity would require a larger response.

Spinning or non-spinning reserve would be used to compensate for significant sources of uncertainty, such as the loss of a generator and more recently a large drop in solar production. Spinning reserve is defined as generators that are in sync with the grid and can provide a response within ten minutes (5.1), (5.2). Non-spinning reserve consists of generators that are not connected to the grid, but can reach a grid-ready state within ten minutes (5.3). Both of these types of reserve are used when there is a contingency in the grid (both renewable and otherwise). They can replace AGC if needed, and are replaced with additional reserve within 30 minutes called replacement reserve.

There are many ways to write the reserve requirements for spinning and non-spinning reserve. Each operating region can enlist its own rules and practices. Many simply include the loss of the single largest generator (5.4). Others include a percentage of total demand and/or non-firm (interruptible) imports (5.5). California ISO includes 5%

of hydro generation and 7% of non-hydro generation (5.6). NREL has proposed a rule that includes 3% of demand and 5% of renewable energy (5.7).

$$r_{g,T}^{SP} \leq u_{g,T} P_g^{max} - P_{g,T}, \ \ \forall g, T \tag{5.1}$$

$$r_{g,T}^{SP} \leq R_g^{10} u_{g,T}, \ \ \forall g, T \tag{5.1}$$

$$r_{g,T}^{NSP} \leq R_g^{10}\left(1 - u_{g,T}\right), \ \ \forall g, T \tag{5.3}$$

$$\sum_{\forall g}\left(r_{g,T}^{SP} + r_{g,T}^{NSP}\right)_{v1} \geq u_{g,T} P_g^{max}, \ \ \forall g, T \tag{5.4}$$

$$\sum_{\forall g}\left(r_{g,T}^{SP} + r_{g,T}^{NSP}\right)_{v2} \geq \alpha \sum_{i \in BUS} d_{i,T} \ + P_T^{non-firm}, \ \ \forall T \tag{5.5}$$

$$\sum_{\forall g}\left(r_{g,T}^{SP} + r_{g,T}^{NSP}\right)_{v3} \geq 0.05 \sum_{g \in GEN} P_{g,T}^{hydro} + 0.07 \sum_{g \in GEN} P_{g,T}^{non-hydro}, \ \ \forall T \tag{5.6}$$

$$\sum_{\forall g}\left(r_{g,T}^{SP} + r_{g,T}^{NSP}\right)_{v4} \geq 0.03 \sum_{i \in BUS} d_{i,T} + 0.05 \sum_{i \in BUS} P_{i,T}^{renewable}, \ \ \forall T \tag{5.7}$$

Any of the rules can be used to plan for uncertainty and ensure there is a reserve buffer that will allow a system to survive a contingency without lost load. However, the use of reserve requirements does not model uncertainty explicitly, which will ultimately give an overly conservative solution. There are alterative methods to deal with uncertainty that attempt to directly address the type of uncertain parameters. While reserve requirements can be written with a specific contingency in mind, they still are not fully sufficient on their own to address uncertainty.

2) Robust Programming

Robust optimization is a method of uncertainty programming that will provide an optimal solution for a group of uncertainties. Optimality can be achieved for any realization within a defined uncertainty set for the problem. The amount of information in the set can vary; often a range and mean will suffice. Reference [12] argues that having a

solution that can withstand a range of possible outcomes is especially relevant for power systems applications due to the high cost of infeasible solutions. The cost of shedding customers is high and will continue to grow. Protection against the risk of load shedding can be worthy of a more conservative generator schedule. Additionally, robust optimization is often more computationally tractable than two-stage scenario based stochastic programs, which makes it an attractive technique for complex problems.

For uncertainty due to solar, a robust uncertainty set can be composed of a range of possible forecast errors for each period. A solution to such a problem is guaranteed to be feasible for all possible forecasts within that set and across time. This type of solution would be apropos if the solar forecast were known to be, for instance, sunny. There might be some slight variations throughout the day that a robust uncertainty set would capture and account for in its solution. However, if a cloud covered the panels and production dropped to zero, the solution would likely no longer be feasible. Any extension of the set to include such events would likely make the solution unnecessarily conservative. For this reason among others, robust optimization was not used for this model.

3) Fuzzy Programming

Fuzzy programming attempts to deal with uncertainty by means of semantics and linguistics. As opposed to well-defined problems that have "crisp" parameters and variables, many decisions need to be made with vague and ambiguous, or "fuzzy" information. There are some problems in power systems that take advantage of fuzzy sets as discussed in Chapter III. Other research has specifically focused on the issue of renewable energy with possibility-based ambiguity [64] for an electric grid; similar to [6], a possibility distribution can be assigned to solar irradiance data and load capacity of

a generator. If a long-term outlook is sought or a planning model was being created, there might be more ambiguity over the amount of solar irradiance present. In a day-ahead framework, it is possible to use forecasting tools to ascertain a degree of certitude that makes fuzzy programming superfluous. While useful for some power systems applications, day-ahead solar generation is better suited for other types of mathematical programming.

4) Stochastic Programming

In a stochastic program, uncertainty is approximated with probability distributions for the uncertain variables or parameters. If the probable set of outcomes is finite, then a stochastic program can be created where the solution is the expected value of the objective. Practically, it is sometimes difficult to establish a probability distribution for the scenarios that accurately reflects the uncertainty. Additionally, a robust solution might require a large number of scenarios, which adds to the computational burden of the problem. However, if the probability set can be created with some confidence, then stochastic programming will return a more efficient solution than other programming methods.

Solar is well suited for stochastic programming due to its probabilistic nature. Large amounts of historical data can help determine reasonable probability distributions that can be tested in actual systems. Once a set of scenarios is created, they can be assigned a set probability, which is used to determine the expected value of the objective cost function.

Due to the limited number of scenarios that can be included in any one stochastic optimization problem, a method to validate the solution is necessary. One drawback to

stochastic programming is the possible infeasibilities that might occur if the actual irradiance drifts far from the forecast or scenarios. To prevent, or at least predict such an event, validation is crucial. The solution should be compared to a large number of additional possible scenarios (forecasts). These results can help a decision maker evaluate the quality of the stochastic solution. Many point to this inflexibility as a fault of stochastic programming; however, it is more so the case that those using stochastic optimization do not further validate their results. With validation, stochastic programming provides efficient and reliable solutions. The validation done for this research is discussed in Chapter VII-B.

B. Scenario Selection

The quality of the solution of a stochastic programming problem is partially dependent on the input scenarios. There are many ways to generate or select scenarios for stochastic programming; some methods might be transferrable between types of input information, but solar is a particular case that requires special attention.

There are two distinct aspects of the solar scenarios that will be addressed: variability and uncertainty. Within seconds or minutes, solar generation can change from a peak to a third of its production, or even near zero production if a large cloud passes overhead. This type of change demonstrates the variability of solar power; Fig. 1 shows an example of solar variability throughout the day from the historical dataset found in [65]. In order to generate scenarios that are true to solar generation patterns, this oscillatory behavior should be taken into account. Following the method developed by Pacific Northwest National Laboratory (PNNL) in [28], historical data was transformed in order to ensure that realistic variability was included in the scenarios. Additionally,

specific mathematical modeling was implemented to ensure that inter-hour variability is reflected in the resulting schedule. This will be further explained in the following section and in Chapter VI-C.

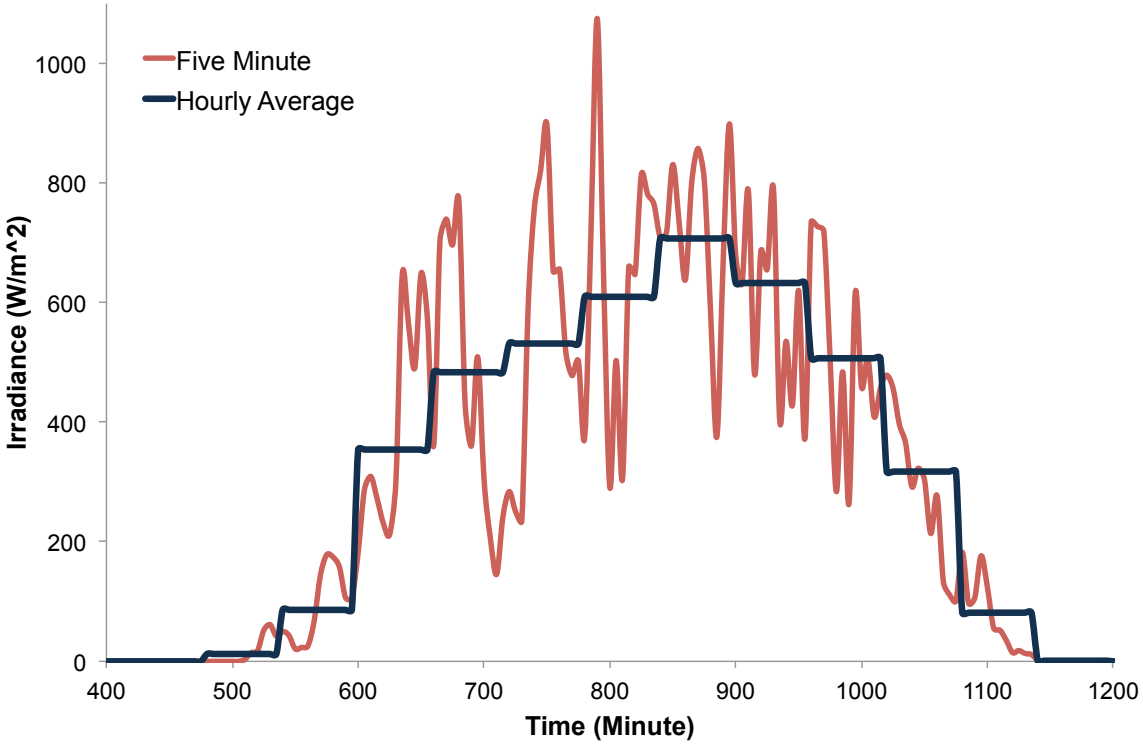

Fig. 1 Variability in solar irradiance data from El Paso, TX

Variability deals with the ability of solar power to change on small times-scales, while uncertainty deals with not knowing the future output. Fig. 2 shows examples of different scenarios for solar generation. Uncertainty dictates that it is unknown which of the outcomes might occur; however, probabilities can be assigned to the likelihood of each scenario. In order to deal with uncertainty, this research utilizes stochastic programming, the details of which were discussed in the last section.

Renewable generation forecast errors are often grouped together. Many have developed methods for dealing with renewable energy that treat wind and solar in the

same way, or solely focus on wind generation in their simulations. However, solar forecast errors are bound by different limits than wind. Solar output has a stricter upper bound; whereas the wind might intensify, solar irradiance cannot increase beyond extraterrestrial solar radiation. Solar output also has the possibility of dropping significantly, possibly to zero, if a cloud that passes overhead; wind is less likely to drop off as quickly or as frequently. Given these characteristics of solar, it is important to treat it with a solar-specific methodology. The chosen procedure for solar scenario generation is outlined in [28]. The method is also explained and utilized in [21], [23], [67], [38].

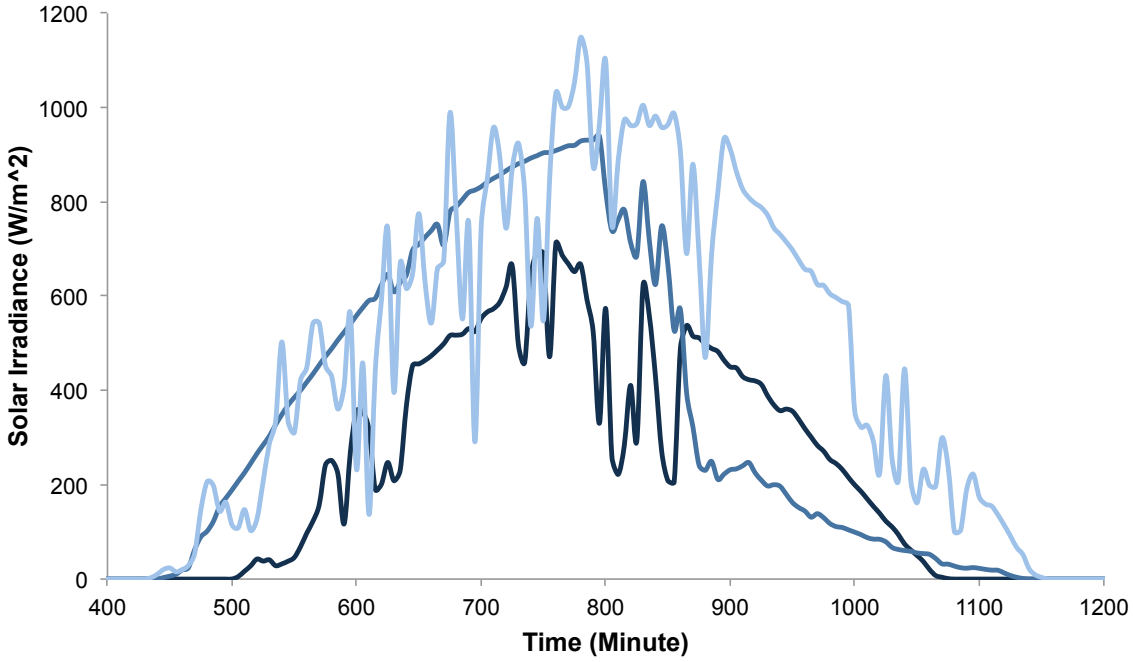

Fig. 2 Solar generation from four days in March 2000

This procedure, developed by PNNL, begins by synthesizing 1-minute historical data obtained from Sacramento Municipal Utility District (SMUD). Using a large amount of data allowed them to generate multiple data for solar plants in their study. Although there are different buses in the network used in this research, a single set of solar

scenarios was developed and scaled according to the peak generation at each bus. The next step in their procedure was developing statistical characteristics of the solar forecast error to be used in a day-ahead framework. They use the notation P_a to represent the actual historical data and P_{max} to represent the ideal maximum solar generation. The maximum will change throughout the year depending on the relative location of the solar measurement units. P_{max} can be considered the solar output if there are no disturbances in the sky, such as clouds or dust, for the time of year of the given data set. This method uses a clearness index level to categorize different time segments of historical data. In order to create a clearness interval, the actual historical data was divided by an ideal sunny forecast, shown in (5.8).

$$CI_t = \frac{P_{a,t}}{P_{max,t}}, \quad \forall t \tag{5.8}$$

A high clearness index indicates that the actual solar data varied little compared to the maximum. A low index shows that there was high variability between the actual data and maximum level. The clearness index cannot exceed one, implying that the actual historical data cannot exceed the maximum solar level for that period. With perfect data, this assumption might hold. However, the data in this research obtained from the NREL CONFRRM network [65] does not contain maximum solar irradiance information (P_{max}). There were many instances in the historical data when the irradiance level exceeded the expected maximum. Fig. 3 shows several examples of such cases. These instances can be explained by the albedo effect; if solar irradiance is reflected by a light colored surface, the irradiance measured below is often intensified beyond the amount that penetrated the atmosphere. Therefore, the ground solar irradiance level will increase beyond the expected maximum for that time period. While this phenomenon was

observed in the data, it was not reflected in the procedure from PNNL. Therefore, the periods where the actual data exceeded the maximum were set to a clearness index of one.

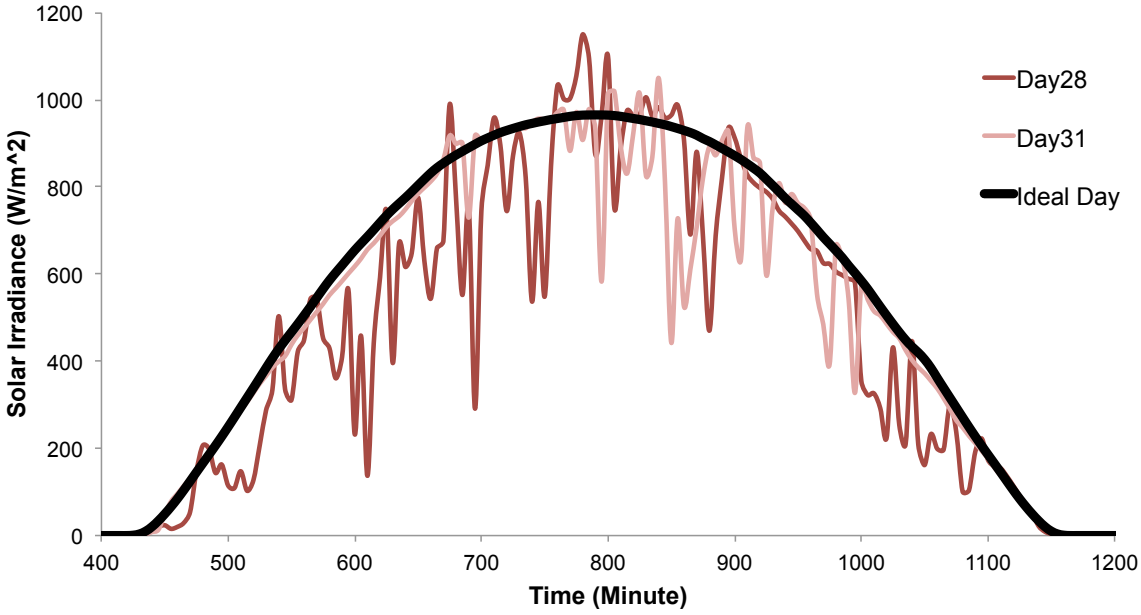

Fig. 3 Three days where solar irradiance exceeds ideal (sunny) irradiance data or P_{max}

Solar forecast errors must be generated in order to create solar output scenarios. The procedure developed by PNNL defines the error with (5.9). At night, the error is always zero, since the solar forecast is zero. It is important to note that $P_{a,t} - P_{max,t}$ can be non-positive, meaning the forecast error can dip below the actual data. When the forecast error is small (near zero) the clearness index will be close to one; this can occur on sunny days with little chance of clouds or on cloudy days when the chance of direct sun is small. The solar forecast errors are generated with an unbiased truncated normal distribution. The variance of the function was derived in [28], and shown in (5.10) where $\phi(\cdot)$ is the probability density function and $\Phi(\cdot)$ is the cumulative distribution function.

Once the clearness index and error limits have been calculated, a four-part procedure can be followed to calculate the errors.

$$\varepsilon_{min,t} = P_{a,t} - P_{max,t} \leq \varepsilon_t \leq \varepsilon_{max,t} = P_{a,t} \tag{5.9}$$

$$std^2(\varepsilon|\varepsilon_{min} < \varepsilon < \varepsilon_{max}) =$$

$$\sigma\left[1 + \frac{\frac{\varepsilon_{min}-\mu}{\sigma}\phi\left(\frac{\varepsilon_{min}-\mu}{\sigma}\right) - \frac{\varepsilon_{max}-\mu}{\sigma}\phi\left(\frac{\varepsilon_{max}-\mu}{\sigma}\right)}{\Phi\left(\frac{b-\mu}{\sigma}\right) - \Phi\left(\frac{\varepsilon_{min}-\mu}{\sigma}\right)} - \left(\frac{\phi\left(\frac{\varepsilon_{min}-\mu}{\sigma}\right) - \phi\left(\frac{\varepsilon_{max}-\mu}{\sigma}\right)}{\Phi\left(\frac{\varepsilon_{max}-\mu}{\sigma}\right) - \Phi\left(\frac{\varepsilon_{min}-\mu}{\sigma}\right)}\right)^2\right] \tag{5.10}$$

First, the clearness index is established with (5.8). The historical data from NREL was on a 5-minute basis. This procedure specifies that the clearness index be calculated using the hourly average, which is appropriate because the eventual forecast will be used in an hourly day-ahead framework. The data was averaged over the hour and then used in (5.8). Second, the clearness index should be divided into four levels, shown in Table I. Each of these levels indicates different kinds of variability. A period that is calculated to be in level 4 will have lower variability than level 1, since it is closer to the maximum/ideal day. Third, the standard deviations for each period will be used to calculate random numbers using the truncated normal distribution from [68]. Lastly, the random numbers will be used as forecast errors for the appropriate periods.

TABLE I CLEARNESS INDEX LEVELS FROM [28]

Level	Clearness Index
1	$0 \leq CI \leq 0.5$
2	$0.2 < CI \leq 0.5$
3	$0.5 < CI \leq 0.8$
4	$0.8 < CI \leq 1.0$

Historical data was used as the basis for the scenarios used in this research. Several characteristic days were chosen as base days for the procedure described above.

Monte Carlo simulations were done to create a large set of scenarios for the analysis. Different classifications of days were assigned probabilities in the simulations, based on their likelihood of occurrence. The forecast error rightly takes into account the variability of solar, and creates scenarios that can be used in stochastic programming.

VI. Day-Ahead Scheduling for Neighboring Systems

The goal of this model is to address the challenge of increased uncertainty due to solar power generation, and demonstrate how a microgrid can ensure reliability and decrease costs in those circumstances. Due to the small size of microgrids, a more detailed relationship can be modeled between the microgrid and its neighboring system. In order to characterize the issues that arise in the microgrid, a two-pronged approach is utilized; a complex mathematical formulation and intricate main–grid microgrid interactions were developed.

A. Description of the Model

The model is intended to replace traditional unit commitment models in day ahead planning. In Fig. 4, a timeline for day-ahead scheduling or planning is presented. Energy bids and load forecasts are fed into a security-constrained UC (SCUC) problem, which is run with hourly periods for the following day. Select contingencies, such as line or generator outages, are then analyzed, i.e., contingency analysis is performed, followed by an ac feasibility check. Once the schedule is determined to be feasible, the final day-ahead schedule is determined. The model described in this section is intended to expand the traditional SCUC problem to be a stochastic SCUC using five-minute periods. This new SCUC is paired with a type of contingency analysis, called solar scenario analysis, which tests the resulting schedule against additional solar forecasts that are not represented in the stochastic programming formulation for the SCUC. After executing these two models, a traditional contingency analysis, ac feasibility checks, and a real time market can be run.

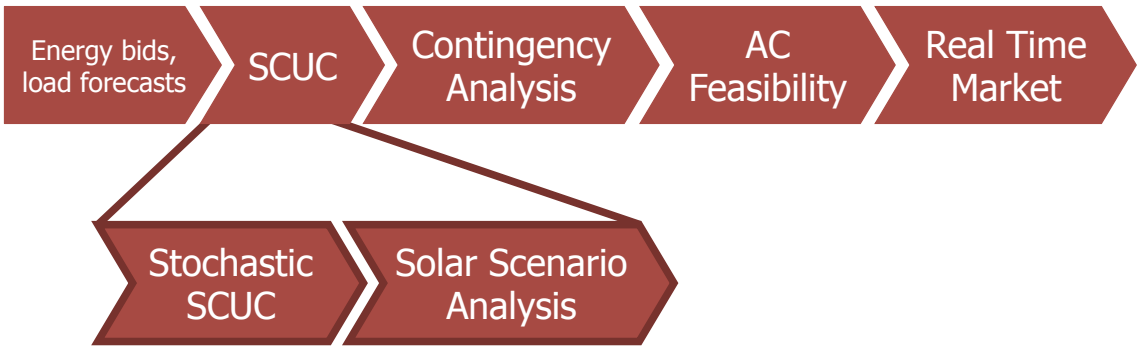

Fig. 4 Timeline for day-ahead planning

Additional modifications are made to the traditional SCUC. This work also extends the SCUC formulation to incorporate a model incorporating the interactions between neighboring systems. The interactions modeled between the main-grid and the microgrid equitably preserve the main-grid's operations, while optimizing the microgrid's resources to deal with PV uncertainty. Trading is allowed on any of the four intertie lines between the main-grid and the microgrid. Trading can be firm, which is defined as guaranteed delivery, or non-firm, which allows the sender to interrupt the power delivery if needed. With this ability, the microgrid is able to disrupt power being sent to the main-grid if a PV contingency occurs, allowing them to avoid turning on an emergency generator or facing a blackout. The trade between the two systems, which enables reserve sharing, will create an improved dispatch that will increase reliability for both grids.

Loop flow and wheeling can often be problems in neighboring systems. Since power follows Kirchhoff's laws, the transmission network in a microgrid might be used as a passageway to get power from one side of the surrounding network to the other. This degrades the transmission lines and can cause unnecessary congestion within the

microgrid. The microgrid can always exist in an islanded mode to avoid this; however, this will likely increase costs for both the main- and microgrid. The system modeled takes advantage of transmission switching, which allows the solver to choose the optimal intertie line schedule. With only one line connected trading can occur and loop flow is eliminated, since the exchange of power can be directly controlled. In this model, there is the possibility to keep all intertie lines open or closed; this allows the model to choose an optimal solution that benefits the microgrid, while maintaining an upper bound for the main-grid's operating cost. Details of the formulation will be described in Part C of this chapter.

In a day-ahead framework, there can be a great deal of uncertainty in the solar forecast. To account for this uncertainty, the model uses solar scenarios created from historical data from NREL's CONFRRM network in El Paso, TX as described in Chapter V-B. The data was sampled on a 5-minute basis and showed a significant amount of variability throughout the hour as seen in Fig. 5. When averaged over the hour for use in day-ahead unit commitment, much of the variability was lost. Additional modeling was added so that the solar scenarios and accompanying power dispatch variables were set over a 5-minute period, whereas the commitment variables were set over an hour period. By having two time periods, the system would be able to account for sudden variations in solar output, while still operating within the bounds of traditional commitment models.

As discussed in Chapter V on uncertainty modeling, stochastic programming best suits solar power generation. The model takes advantage of seven solar scenarios, generated from the method described in Chapter V-B. All of the components described above were written into a stochastic mixed integer linear program. Using A Mathematical

Programming Language (AMPL), attempts were made to find an optimal solution for the problem. After several different techniques were attempted, it was apparent that it was too large and complex to solve in one model. Due to these complexities, a decomposition technique was utilized.

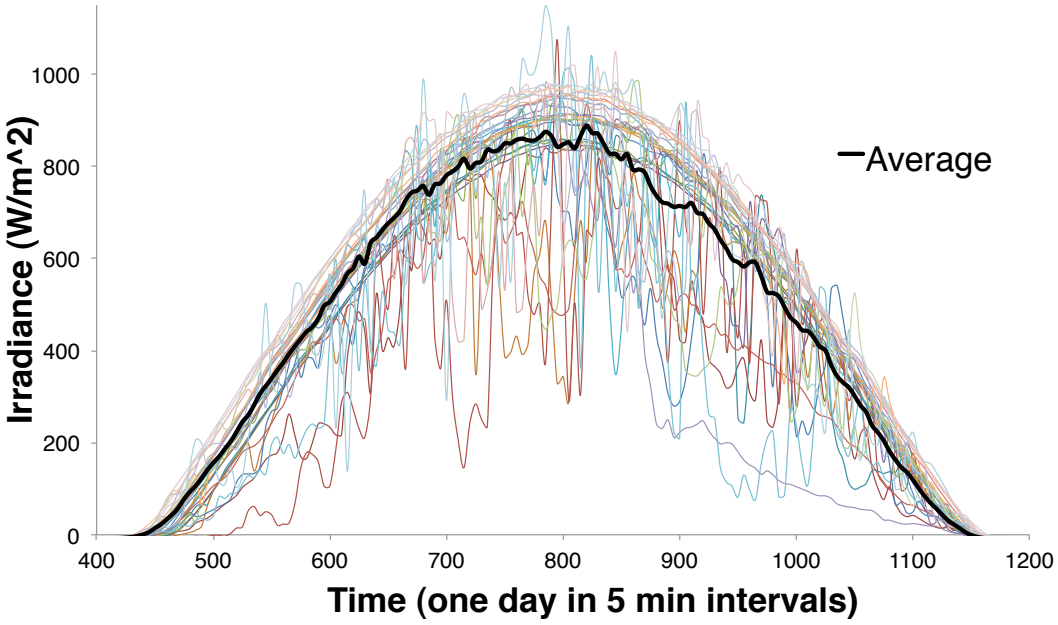

Fig. 5 Solar irradiance data from El Paso, TX

B. Benders' Decomposition

Benders' decomposition is a well-researched and often utilized decomposition technique for integer and mixed integer linear programs [69]. Instead of solving one large complex problem, it breaks the problem into smaller component parts and solves them individually. The goal of such an approach is to ease the computational burden; however, depending on the problem, this maybe not always be the case. In Benders' approach, the problem is split into a master problem and a subproblem. The master problem is an integer or mixed integer problem, which fixes particular variables for the subproblem.

The subproblem then solves a linear program using the fixed variables and adds constraints to the master problem to reflect the added complexity of the subproblem. This process then iterates back and forth until the convergence criteria is reached.

The basic premise of Benders' decomposition is that a mixed integer problem can be reformulated into a problem that is supposed to be easier to solve than the original. A full proof of this reformulation can be found in [70]. What follows is a simple statement of the reformulation. Assuming a mixed integer problem

$$\min c^T x + h^T y \tag{6.1}$$

Subject to

$$Ax + Gy \leq b \tag{6.2}$$

$$x \in X \subseteq Z_+^n, y \in \mathbb{R}_+^p \tag{6.3}$$

where x is a vector of integer variables, y is a vector of continuous variables, A, G are matrices and c, h, b are vectors with complementary dimensions, Z_+^n is the set of n-dimensional nonnegative integral vectors, and $\mathbb{R}_+^p$ is the set of p-dimensional nonnegative real vectors. The problem can be reformulated as

$$\min \eta \tag{6.4}$$

Subject to

$$\eta \geq c^T x + u^k(b - Ax), \ \forall k \in K \tag{6.5}$$

$$v^j(b - Ax) \geq 0, \ \forall j \in J \tag{6.6}$$

$$x \in X, \eta \in R^1 \tag{6.7}$$

where u^k is a set of K-dimensional extreme points and v^j is a set of J-dimensional extreme rays.

Equations (6.4)-(6.7) are not a linear program, but can be solved as a mixed integer program (MIP) with complicating variables and a linear program (LP). The LP adds new constraints to the MIP at each iteration, making Benders' decomposition a row generation method. Details about the algorithm can be found in [70], including characteristics of the relationship between the LP and MIP. When solving these problems, the MIP is solved with no initial conditions, and the solution is passed to the LP. If the MIP is infeasible, then the original problem is infeasible; however, if it is unbounded, then a feasible solution with a reasonable (predetermined) initial objective should be sent to the LP. The LP then solves using the fixed integer values from the MIP. If the LP solution reaches negative infinity (for a minimization problem), then the original problem is unbounded. If it is infeasible, the dual problem has an unbounded solution and a feasible region exists along an extreme ray that is unbounded. The extreme ray is added to the MIP with $v^j(b - Ax) < 0$, often called a feasibility cut. If the problem is finite, then the solution can be tested for optimality. If the objective of the LP is less than the objective of the MIP (for a minimization problem), then the solution is an optimal solution for the whole problem. If the LP objective is greater than the MIP, an extreme point will be generated and added as an optimality cut to the MIP.

There are several issues with Benders' decomposition method. Benders' is intended to solve a complex problem more efficiently by separating it into two stages. The iterative process can sometimes cause the master MIP problem to bloat with too many constraints, slowing down solution times. Therefore, if not formulated properly, Benders' could take longer to solve than a single MIP problem. Benders' can be parallelized and does converge quickly in many cases. Some problems might not fit into a

Benders' framework because the constraints must be L-shaped and the subproblem must be convex. The UC problem, however, does fit into this formulation well as evidenced by the literature in Chapter III. The following paragraphs will discuss the formulation as it applies to this problem.

Unit commitment problems are well suited for Benders' decomposition with examples in [71], [72], [73] and a survey done in [74]. The master (MIP) problem is frequently composed of the UC problem without transmission constraints. The complicating variables are the binary on/off generator commitment variables. The generation schedule is fixed in the master and passed to the subproblem, which has transmission constraints. The problem can be an economic dispatch problem or an optimal power flow problem, depending on the formulation of the master.

The problem described in Chapter VI-A was decomposed in a similar way. The master problem is a unit commitment problem, including transmission constraints and several other complicating variables. Transmission switching, intertie line imports, and reserve requirements are also included as constraints in the master problem. Once an optimal solution is reached, the generation schedule, the status of the intertie lines (open/closed) and the import level (in MW) are passed to the subproblem. The subproblem is built on a DCOPF framework with the addition of solar scenarios, making it a stochastic linear program. The cuts are then passed back to the master problem until convergence is reached. Convergence is defined as the iteration at which the subproblem's objective is lower than the master problem objective. At this point, the master problem has found a solution that accounts for the additional cuts (costs) from the subproblem. Benders' can be especially useful because contingencies from the master

problem are dominated by those in the subproblem. The master problem solution accounts for the worst-case violation, which is taken care of in the subproblem instead of the master.

As discussed above, there are two primary types of cuts for Benders' decomposition: feasibility cuts and optimality cuts. In this problem, feasibility in the LP was ensured through slack variables for demand and solar generation. The slack variable for demand was allowed to vary from the demand level to zero (meaning there is no demand in the system). The solar slack variable was allowed to vary from the peak solar injection to zero, and was also indexed by scenario. Due to the sometimes large variability between scenarios, solar curtailment could vary when the scenario differed greatly from the average used in the master problem. Optimality cuts are applied at ever iteration of the problem through the dual formulation of the LP. Essentially, these cuts add a cost to the MIP for the complexity in the LP. The cut is composed of the dual variable for each constraint in the LP multiplied by the right-hand-side (parameters) of the constraint. Sometimes, the right-hand-side values in the subproblem contain fixed values from the master. Therefore, when applied back to the master, the value becomes unfixed and is able to take on a new value.

In order to account for the desired amount of complexity, the problem was divided into three stages as seen in Fig. 6: a system-wide UC problem, a microgrid UC problem (the master), and a system-wide OPF (the subproblem). The first stage is a simple problem that establishes the operating costs of the main-grid without the influence of trading from the microgrid. This stage sets an upper bound on the main-grid's costs and a base level for power flows on the intertie lines. It sets a precedent for what would

occur if the system where optimized as a whole, instead of as two individual systems. This multi-stage structure is used to model the developed interactions with the microgrid and the main-grid appropriately. The second stage structure ensures Pareto-improvements are achieved for both systems using the information gained in stage one. This allows the microgrid to improve its ability to predict operating conditions for the main-grid and, hence, trading opportunities for both energy and ancillary services. Additional modeling was used to ensure that uncommitted non-spinning generators would be available for use in the third stage OPF.

The third stage uses solar scenarios to capture forecast uncertainty. Since the microgrid has high levels of variable renewable resources, day-ahead planning that considers only hourly periods will result in high real-time re-dispatch costs to correct for the variability and uncertainty. Stage three, which has 5-minute periods, uses penalty factors for each five-minute period to capture the true costs for deviating away from the planned schedule.

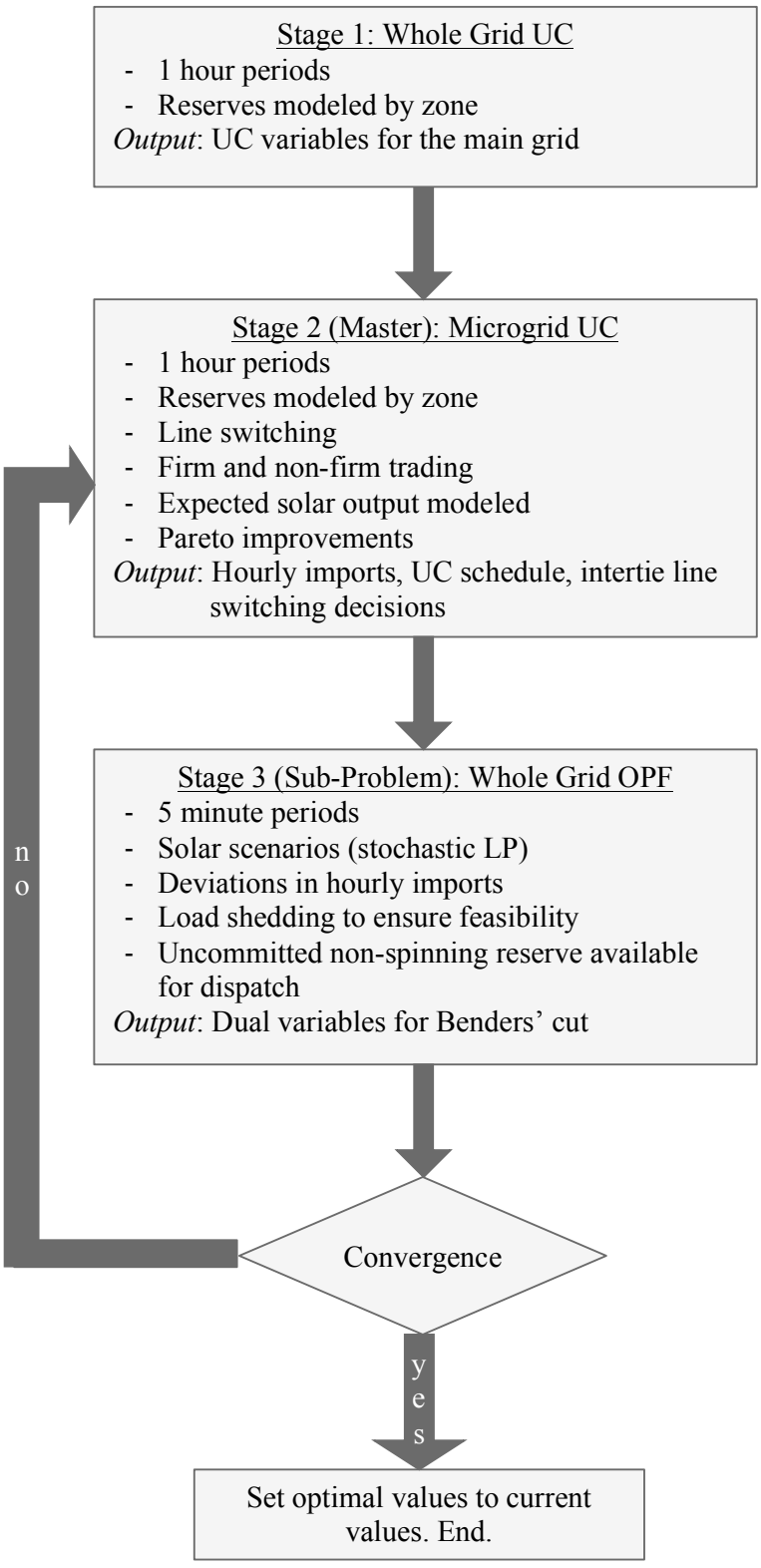

Fig. 6 Three stage day-ahead scheduling process

C. Mathematical Formulation

As described in the previous section, the formulation is divided into three stages. The first stage is independent of stages two and three, which are the master and subproblem of Benders' decomposition respectively. Once the first stage finds an optimal solution, certain variables are fixed and used as parameters in the following two stages. The framework for each stage is described in the following three subsections. In this chapter, *g* and *GEN* refer to all generators in both the main-grid and the microgrid. When the main- or microgrid is specifically used, *MICRO* and *MAIN* will be designated.

1) Stage One

In stage one, a day-ahead unit commitment model is run for the main- and microgrid. The objective of stage one is to minimize operating costs for both systems. The formulation is very similar to the general UC formulation explained in Chapter IV-B. Generator, line, and angle limits are shown in (6.9)-(6.11), and (6.12) is a dc power flow approximation. Equations (6.13)-(5.15) define the startup and shutdown variables. The generator ramp rates and minimum up and down times are described in (6.16)-(6.19) respectively.

Spinning and non-spinning reserve requirements are outline in (6.20)-(6.26). The requirements are based on NREL's requirement for operating reserve, which dictates that reserves should cover 3% of load and 5% of variable or renewable generation . The reserve requirements also stipulate that operating reserve must exceed the largest single generator outage. Due to the microgrid's small size, the values used in (6.23) and (6.24) are more conservative than NREL's rule. Choosing higher values helps to ensure that load shedding will not occur and also speeds up convergence. The α associated with load

is 5% and the β associated with solar is 20%. Finally, the node balance constraint is found in (6.27). The solar forecast used in (6.27) is the hourly average of the scenarios used in stage three. There is no trading or transmission switching allowed in order to determine the main-grid's anticipated operation cost and the amount of power flowing into the microgrid.

$$\min \sum_{\forall T \in HOUR} \sum_{\forall g \in GEN} \left(c_g P_{g,T} + c_g^{SU} v_{g,T} + c_g^{NL} u_{g,T} \right) \tag{6.8}$$

Subject to

$$u_{g,T} P_g^{min} \leq P_{g,T} \leq u_{g,T} P_g^{max}, \ \ \forall g, T \tag{6.9}$$

$$P_k^{min} \leq P_{k,T} \leq P_k^{max}, \ \ \forall k, T \tag{6.10}$$

$$\theta^{min} \leq \theta_{n,T} - \theta_{m,T} \leq \theta^{max}, \ \ \forall k, T \tag{6.11}$$

$$P_{k,T} = B_k \left(\theta_{n,T} - \theta_{m,T} \right), \ \ \forall k, T \tag{6.12}$$

$$v_{g,T} - w_{g,T} = u_{g,T} - u_{g,T-1}, \ \ \forall g, T \tag{6.13}$$

$$0 \leq v_{g,T} \leq 1, \ \ \forall g, T \tag{6.14}$$

$$0 \leq w_{g,T} \leq 1, \ \ \forall g, T \tag{6.15}$$

$$P_{g,T} - P_{g,T-1} \leq R_g u_{g,T-1} + R_g^{SU}(v_{g,T}), \ \ \forall g, T \tag{6.16}$$

$$P_{g,T-1} - P_{g,T} \leq R_g u_{g,T} + R_g^{SD}(w_{g,T}), \ \ \forall g, T \tag{6.17}$$

$$\sum_{r=T-\tau_g^{UT}+1}^{T} v_{g,r} \leq u_{g,T}, \ \ \forall g, T \tag{6.18}$$

$$\sum_{r=T-\tau_g^{DT}+1}^{T} w_{g,r} \leq 1 - u_{g,T}, \ \ \forall g, T \tag{6.19}$$

$$r_{g,T}^{SP} \leq u_{g,T} P_g^{max} - P_{g,T}, \ \ \forall g, T \tag{6.20}$$

$$r_{g,T}^{SP} \leq R_g^{10} u_{g,T}, \ \ \forall g, T \tag{6.21}$$

$$r_{g,T}^{NSP} \leq R_g^{10} \left(1 - u_{g,T} \right), \ \ \forall g, T \tag{6.22}$$

$$\sum_{\forall g \in GEN} r_{g,T}^{SP} \geq \frac{1}{2}\left[\alpha \sum_{i \in BUS} d_{i,T} + \beta \sum_{i \in BUS} P_{i,T}^{PV}\right], \quad \forall T \tag{6.23}$$

$$\sum_{\forall g \in GEN}\left(r_{g,T}^{SP} + r_{g,T}^{NSP}\right) \geq \alpha \sum_{i \in BUS} d_{i,T} + \beta \sum_{i \in BUS} P_{i,T}^{PV}, \quad \forall T \tag{6.24}$$

$$\sum_{\forall g \in GEN} r_{g,T}^{SP} \geq \frac{1}{2}\left[P_{g,T} + r_{g,T}^{SP} + \beta \sum_{i \in BUS} P_{i,T}^{PV}\right], \quad \forall g, T \tag{6.25}$$

$$\sum_{\forall g \in GEN}\left(r_{g,T}^{SP} + r_{g,T}^{NSP}\right) \geq P_{g,T} + r_{g,T}^{SP} + \beta \sum_{i \in BUS} P_{i,T}^{PV}, \quad \forall g, T \tag{6.26}$$

$$\sum_{\forall k \in \delta^{+}(i)} P_{k,T} - \sum_{\forall k \in \delta^{-}(i)} P_{k,T} + \sum_{\forall g \in g(i)} P_{g,T} + P_{i,T}^{PV} = d_{i,T}, \quad \forall i, T \tag{6.27}$$

2) Stage Two

Stage two includes unit commitment for the microgrid and an optimal power flow for the main-grid. Equations (6.9)-(6.26) from stage one are also included in this stage; however, (6.13)-(6.19) are exclusively for the microgrid since the main-grid's commitment status is fixed after the first stage. The objective of stage two is to minimize η, which is determined by constraints (6.29) and (6.30). It is first bounded by the original objective of the problem, which was a combination of Stages 2 and 3 (the master and subproblem). This objective minimized operating costs, the difference of power sold and purchased, and a non-spinning adjustment term (described in the next section). The second constraint that impacts η is the Benders' decomposition optimality cut, which sums the fixed costs from the microgrid, the adjustable non-spinning generators, and the product of the duals of the constraints in the subproblem and their right-hand-sides.

Constraints (6.31)-(6.33) deal with the imports coming into and out of the microgrid. The variable P_T^* represents the net hourly imports either purchased or sold from the microgrid to the main-grid. The model was designed so that power can either be purchased or sold during the hour, as indicated by the variable E_T^*, and is bounded by the sum of the maximum intertie line ratings. The reserve requirements defined in stage one

are also adjusted to reflect trading. Non-firm trading can be recalled, and therefore, $P_T^{+NF} + P_T^{-NF}$ is added to the right-hand-side constraints (6.23)-(6.26).

Transmission line switching is described by (6.34)-(6.37); these constraints were developed in [75] and [76] and adapted for this model. Constraints (6.34)-(6.36) ensure that power flow and angle differences between two intertie lines are within the limits if the line is closed or bound by zero if the line is open, designated by $z_{k,T}$. The number of open lines is limited by the parameter C_T in (6.37). The big M value is defined by $M_k \geq B_k\left(\theta_n^{max} - \theta_l^{min}\right)$. Equations (6.38)-(6.41) describe the Pareto improvement for the main-grid. This stage minimizes the microgrid's cost; in order to ensure that the main-grid's dispatch does not change simply to reduce costs in the microgrid, this constraint ensures the main-grid's costs do not increase. The upper bound of the constraint is the sum of the cost to dispatch power in stage one and the potential imports, which is defined as the product of the power flowing on the intertie lines and an import price. Constraint (6.43) is the node balance constraint, which uses an averaged forecast for solar generation.

$$\min \eta \tag{6.28}$$

Subject to

$$\eta \geq \sum_{\forall T \in HOUR}\left(\sum_{\forall g \in MICRO} c_g P_{g,T} + c_g^{SU} v_{g,T} + c_g^{NL} u_{g,T}\right) + \left(c_T^{-F} P_T^{-F} + c_T^{-NF} P_T^{-NF}\right)$$
$$- \left(c_T^{+F} P_T^{+F} + c_T^{+NF} P_T^{+NF}\right) + \sum_{\forall g \in GEN_{fast}} \rho_c\left(c_g^{SU} + c_g^{NL}\right)\left(1 - u_{g,t,c}^{NSP}\right) \tag{6.29}$$

$$\eta \geq \sum_{\forall z \in Z} \lambda_z^y b_z + \sum_{\forall T \in TIME} \sum_{\forall g \in MICRO} c_g P_{g,T} + c_g^{SU} v_{g,T} + c_g^{NL} u_{g,T}$$
$$+ \sum_{\forall g \in GEN_{fast}} \left(\rho_c\left(c_g^{SU} + c_g^{NL}\right)\left(1 - u_{g,T,c}^{NSP}\right)\right), \quad \forall y \tag{6.30}$$

$$\left(P_T^{-NF} + P_T^{-F}\right) - \left(P_T^{+NF} + P_T^{+F}\right) = \sum_{\forall k \in ITIE} P_{k,T}, \quad \forall T \tag{6.31}$$

$$0 \leq P_T^{-NF} + P_T^{-F} \leq \sum_{\forall k \in ITIE} P_k^{max}(E_T^-), \ \ \forall T \tag{6.32}$$

$$0 \leq P_T^{+NF} + P_T^{+F} \leq \sum_{\forall k \in ITIE} P_k^{max}(E_T^+), \ \ \forall T \tag{6.33}$$

$$B_k\left(\theta_{n,T} - \theta_{m,T}\right) - P_{k,T} + \left(1 - z_{k,T}\right)M_k \geq 0, \ \ \forall k, T \tag{6.34}$$

$$B_k\left(\theta_{n,T} - \theta_{m,T}\right) - P_{k,T} - \left(1 - z_{k,T}\right)M_k \leq 0, \ \ \forall k, T \tag{6.35}$$

$$z_{k,T}P_k^{min} \leq P_{k,T} \leq z_{k,T}P_k^{max}, \ \ \forall k, T \tag{6.36}$$

$$\sum_{\forall k \in ITIE}\left(1 - z_{k,T}\right) \leq C_T, \ \ \forall T \tag{6.37}$$

$$\sum_{\forall T \in HOUR} \sum_{\forall g \in MAIN}\left(c_g P_{g,T}\right) - \left(c_T^{-F} P_T^{-F} + c_T^{-NF} P_T^{-NF}\right) + \left(c_T^{+F} P_T^{+F} + c_T^{+NF} P_T^{+NF}\right)$$
$$\leq \left(\sum_{\forall T \in HOUR} \sum_{\forall g \in MAIN}\left(c_g \overline{P_{g,T}}\right) - c_T^{+F}\left(\overline{P_{g,T}^{MAIN}} - \sum_{\forall i \in MAIN} d_{i,T}\right)\right)\zeta_T$$
$$+ (1 - \zeta_T)M^{\zeta}, \forall T \tag{6.38}$$

$$0 \leq \zeta_T \leq 1, \ \ \forall T \tag{6.39}$$

$$\zeta_T \geq E_T^+, \ \ \forall T \tag{6.40}$$

$$\zeta_T \geq E_T^-, \ \ \forall T \tag{6.41}$$

$$u_{g,T} \leq u_{g,T,c}^{NSP}, \ \ \forall g, T, c \tag{6.42}$$

$$\sum_{\forall k \in \delta^+(i)} P_{k,T} - \sum_{\forall k \in \delta^-(i)} P_{k,T} + \sum_{\forall g \in g(i)} P_{g,T} + P_{i,T}^{PV} = d_{i,T}, \ \ \forall i, T \tag{6.43}$$

(6.9)-(6.26)

$$u_{u,T}, z_{k,T}, E_T^+, E_T^- \in \{0,1\}$$

3) Stage Three

Stage three is the subproblem for Benders' decomposition and is, therefore, a linear program. The base model is an OPF for both the main- and the microgrid. While stage one and two were hourly models, stage three is a day-ahead model split into five-minute intervals with 288 periods in total (24 hours x 12 5-minute periods/hour). This

stage uses a smaller timeframe to better capture the variability inherent in solar generation. As is seen by Fig. 1, the variability in solar data cannot be appropriately estimated when considering the impact of an average solar forecast over an hour. Although the problem is computationally intense it is beneficial for the microgrid to plan at this level of detail for solar variability, since it is a small system with limited resources. Accordingly, this stage also presents seven solar scenarios to capture inaccuracies in day-ahead solar forecasts. Once this stage solves, the dual variables are output and utilized in the next iteration of the master problem.

The objective is the sum of the weighted power dispatched, the load shed, and the amount of power that deviates away from the hourly imports fixed from stage two. Load shedding and solar curtailment are added to the node balance constraint (6.43) in order to ensure feasibility in the subproblem. Load shedding has a cost of $833.33 per five-minute period or $10,000 per hour. As solar is a free fuel source, curtailment does not have a cost associated to it. The final terms in the summation in the objective describe the penalty factor (κ) and deviation (Δ) for firm and non-firm imports purchased and sold by the microgrid. The deviation is defined as the absolute change from the hourly averaged import that was temporarily fixed from stage two. The constraints in (6.46)-(6.53) define the bounds; it should be noted that all hourly variables in stage two fixed for stage three have the same value for the 12 five-minute intervals within an hour. The deviations draw attention to discrepancies between the set hourly imports and what might occur due to uncertainty in real-time. These inadequacies can be corrected by changing the hourly import level or taking actions in real-time.

The commitment decisions for the non-spinning generators are made in the master problem, which includes non-spinning adjustment terms that are indexed by scenario. By applying the Benders' optimality cuts back to the master, it appropriately influences the problem to choose non-spinning reserve on a per scenario basis. To do this, additional variables and constraints (non-spinning adjustment terms) were developed to allow non-spinning generation to fluctuate for each scenario. The variable $u_{g,t,c}^{NSP}$ is fixed after stage two and utilized as the non-spinning generators' commitment status in three. The dispatch from these generators, $P_{g,t,c}^{NSP}$, is added to the objective along with the dispatch variable for all generators in the system. $P_{g,t,c}^{NSP}$ is bound the minimum generation capacity and the non-spinning ramp rate for the generator in (6.56).

Finally, the bounds in (6.57) and (6.58) limit the amount of power dispatch discrepancy allowed between scenarios. These constraints ensure that the actual dispatch level cannot vary to extremes between the seven scenarios.

Additional constraints from stages one and two are also included with the exception that certain variables are defined over five-minute periods. In the generation capacity, line, and angle limits in (6.9)-(6.11), the variables $P_{g,t,c}$, $P_{k,t,c}$, and $\theta_{l,t,c}$ are determined for 5-minute intervals over the number of scenarios or contingencies (c). The reserve constraints in (6.21)-(6.26) are similarly changed with spinning reserve determined for the average solar scenario for 5 minutes $r_{g,t}^{SP}$ and non-spinning reserve allowed to vary for each scenario $r_{g,t,c}^{NSP}$. The line switching constraints in (6.34)-(6.37) are included in this stage, except the power flow variable is again indexed by scenario and on

a 5-minute interval, and the lines are fixed as either open or closed (determined in stage two).

$$\min \ \sum_{\forall t \in MIN} \sum_{\forall c \in SCEN} \rho_c \left(\sum_{\forall \in GEN} c_g \left(P_{g,t,c} + P_{g,t,c}^{NSP} \right) + \ c^{LS} S_{i,t} + \ (\Delta_t^{+F} \kappa_t^{+F} + \right.$$

$$\left. \Delta_t^{+NF} \kappa_t^{+NF} + \Delta_t^{-F} \kappa_t^{-F} + \Delta_t^{-NF} \kappa_t^{-NF}) \right) \tag{6.44}$$

Subject to

$$(P_t^{-NF} + P_t^{-F}) - (P_t^{+NF} + P_t^{+F}) = \sum_{\forall k \in ITIE} P_{k,t,c}, \ \ \forall t \tag{6.45}$$

$$\Delta_t^{-NF} \geq \left(P_t^{-NF} - \overline{P_T^{-NF}} \right), \ \ \forall t \tag{6.46}$$

$$\Delta_t^{-NF} \geq \left(\overline{P_T^{-NF}} - P_t^{-NF} \right), \ \ \forall t \tag{6.47}$$

$$\Delta_t^{-F} \geq \left(P_t^{-F} - \overline{P_T^{-F}} \right), \ \ \forall t \tag{6.48}$$

$$\Delta_t^{-F} \geq \left(\overline{P_T^{-F}} - P_t^{-F} \right), \ \ \forall t \tag{6.49}$$

$$\Delta_t^{+NF} \geq \left(P_t^{+NF} - \overline{P_T^{+NF}} \right), \ \ \forall t \tag{6.50}$$

$$\Delta_t^{+NF} \geq \left(\overline{P_T^{+NF}} - P_t^{+NF} \right), \ \ \forall t \tag{6.51}$$

$$\Delta_t^{+F} \geq \left(P_t^{+F} - \overline{P_T^{+F}} \right), \ \ \forall t \tag{6.52}$$

$$\Delta_t^{+F} \geq \left(\overline{P_T^{+F}} - P_t^{+F} \right), \ \ \forall t \tag{6.5}$$

$$0 \leq P_t^{-NF} + P_t^{-F} \leq \sum_{\forall k \in ITIE} P_k^{max} \left(\overline{E_t^{-}} \right), \ \ \forall t \tag{6.54}$$

$$0 \leq P_t^{+NF} + P_t^{+F} \leq \sum_{\forall k \in ITIE} P_k^{max} \left(\overline{E_t^{+}} \right), \ \ \forall t \tag{6.55}$$

$$\left(1 - \overline{u_{g,t,c}^{NSP}} \right) P_g^{min} \leq P_{g,t,c}^{NSP} \leq R_g^{NSP} \left(1 - \overline{u_{g,t,c}^{NSP}} \right), \ \ \forall g, t, c \tag{6.56}$$

$$P_{g,t,0} - P_{g,t,c} \leq R_g^{scen} \, \overline{u_{g,t}}, \ \ \forall g, t, c \tag{6.57}$$

$$P_{g,t,c} - P_{g,t,0} \leq R_g^{scen} \, \overline{u_{g,t}}, \ \ \forall g, t, c \tag{6.58}$$

$$\sum_{\forall k \in \delta^{+}(i)} P_{k,t,c} - \sum_{\forall k \in \delta^{-}(i)} P_{k,t,c} + \sum_{\forall g \in g(i)} P_{g,t,c} + P_{i,t,c}^{PV} - P_{i,t,c}^{PVcurtail} = d_{i,t} - S_{i,t}, \quad \forall i, t, c \tag{6.59}$$

$$0 \leq S_{i,t} \leq d_{i,t}, \quad \forall i, t \tag{6.60}$$

$$0 \leq P_{i,t,c}^{PVcurtail} \leq P_{i,t,c}^{PV}, \quad \forall i, t, c \tag{6.61}$$

(6.9)-(6.12), (6.21)-(6.26), (6.34)-(6.37)

VII. RESULTS

The model describe in Chapter VI was written in the programming language AMPL. Gurobi, a mathematical programming solver, was used to solve the problem through the AMPL interface. The 1996 Reliability Test System was used to test the model. The one zone network seen in Fig. 7 was divided into two separate networks: a main- and microgrid. The microgrid is composed of four buses (2, 6, 7, 8), with two additional lines to create a meshed system within the microgrid. The main-grid is composed of the remaining 20 buses. The network information was obtained from University of Washington [77]. Solar penetration in the microgrid was 60%.

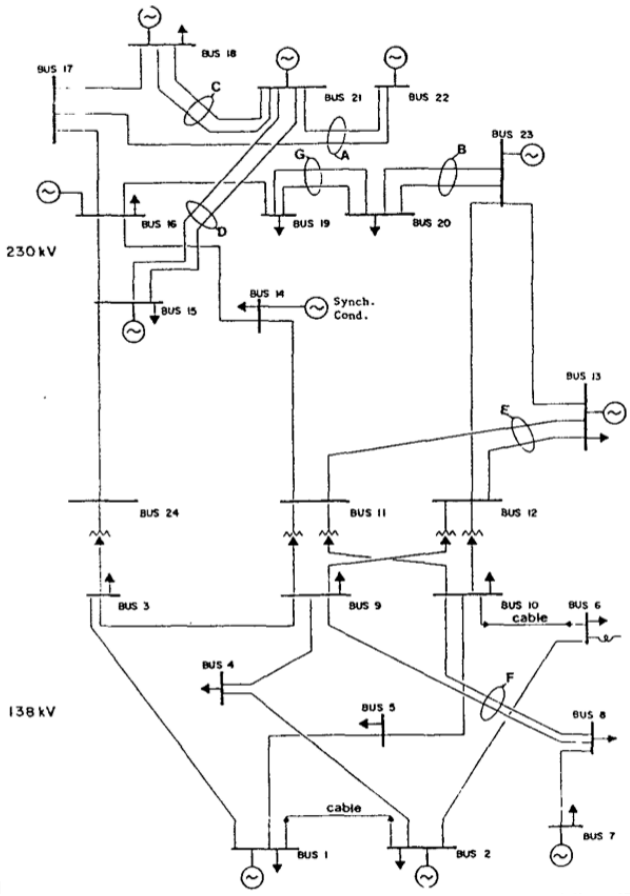

Fig. 7 One zone Reliability Test System – 1996 from [78]

The model was run with an Intel Xeon X5690 CPU at 3.47 GHz on a computer with 48 GB of RAM and 24 cores. The model converged in 63 iterations with a 2% MIP gap in the master problem. Changes to the number and quality of scenario drastically altered the rate of convergence. For use in operations, the number of scenarios can change depending on the desired convergence time. In total, this model ran for 2195 seconds, which is approximately 37 minutes. The total includes the first stage, as well as the 63 iterations of stages two and three.

A. Three Stage Model Results

After simulating this model, the following results have been obtained. Fig. 8 shows the firm and non-firm imports that are purchased or sold by the microgrid. During the evening hours when the generation from solar PV is zero, the microgrid chooses to buy power, most of which is firm (guaranteed) imports. During the middle of the day, the microgrid sells power to the main-grid. About two-thirds of the power sold is non-firm, while the rest is firm. This ratio suggests that the microgrid is relatively certain that it can sell some power to the main-grid during the middle of the day, but still cautious enough to make most non-firm to ensure that it can recall that power if there is a solar contingency. This also requires the microgrid to have more reserves in its system. While solar is ramping up, there is less volatility in the scenarios, which leads to more firm power being sold to the main-grid. However, in the later afternoon, there is a great deal of variability among the scenarios, leading to more uncertainty and non-firm power being sold.

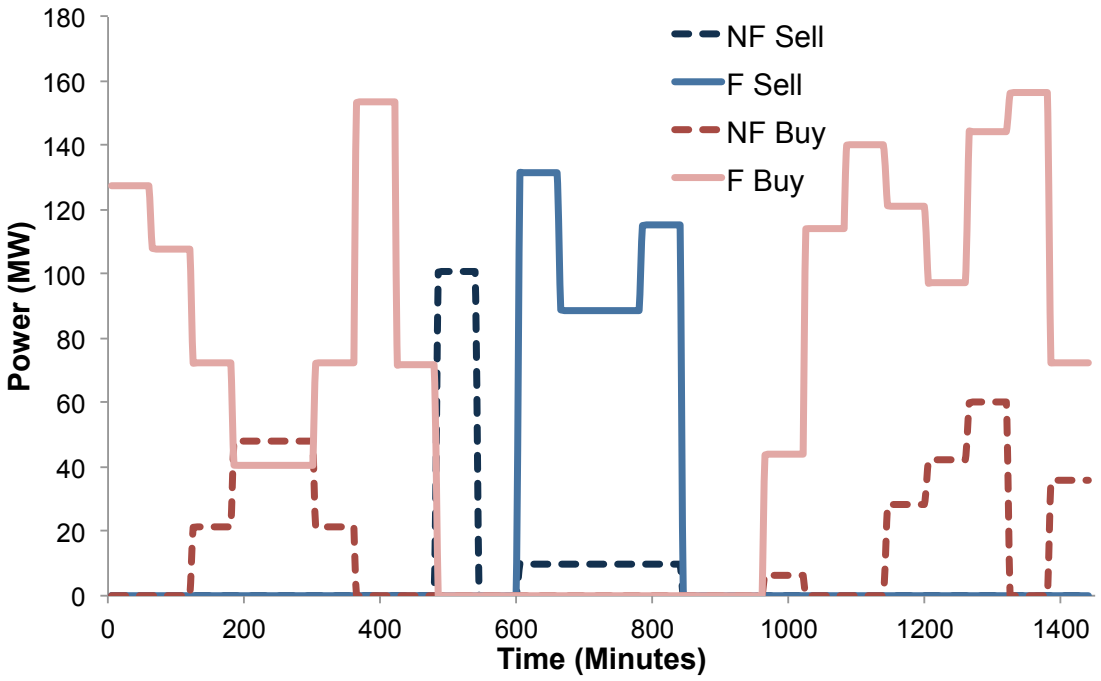

Fig. 8 Firm and non-firm imports purchased or sold from the microgrid to the main-grid

On any given day, the microgrid is likely to face the most uncertainty while solar is ramping up and down in the mornings and afternoons. The load is simultaneously ramping up during the morning, and down after the peak during the later afternoon. In Fig. 9, the number of closed intertie lines is shown in the dark squares. During the morning and midday hours, there are more lines connected between the two systems, thereby allowing more power to be purchased or sold. Interestingly, in hours 17 and 18 there is only one intertie line connected between the main- and microgrid. This is complemented by the low imports in those two hours between the systems in Fig. 8. During this period, demand is ramping up to reach its peak while solar is ramping down. It is possible that, due to the increased strain on the system, the microgrid would prefer to eliminate the chances of loop flow by only allowing one line to be connected. During this

period, the microgrid is producing almost all of the power needed to meet demand and has less need to enter into uncertain non-firm agreements to either buy or sell power.

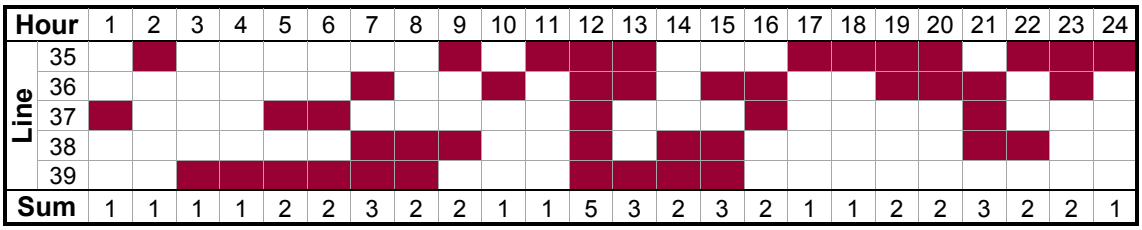

Fig. 9 Switched intertie lines are shown in the dark squares and white squares show open lines

The amount of reserve needed in each system is shown in Fig. 10. During the middle of the day, when solar is almost at its peak, the microgrid's reserve level increases. It is evident from the juxtaposition of the minimum solar level that the microgrid is retaining such high reserves when there is a significant consistent difference between the maximum and minimum scenarios. Due to the five-minute model, the microgrid is also able to capture small drops and sudden changes in solar production through an increased reserve level. Meanwhile, the main-grid is able to keep a fairly consistent reserve level, with a dip in the morning when the microgrid is selling firm power.

In addition to comparing solar production to reserve, it is also worthwhile to examine the import deviations. During the subproblem, imports are allowed to deviate away from the fixed hourly values established in the master problem. The final deviations are shown in Fig. 11, which ranges from approximately 8 AM to 2 PM. Non-firm power sold by the microgrid deviates significantly away from the hourly fixed value at nine o'clock and deviates less for the amount purchased at ten o'clock. This deviation is solely for the non-firm imports, which can be recalled if needed. Instead of paying a penalty in

real-time, the microgrid can simply recall the non-firm imports if there is a contingency. However, the deviations in firm power might need to be addressed by the system operator if there is a solar contingency in real-time.

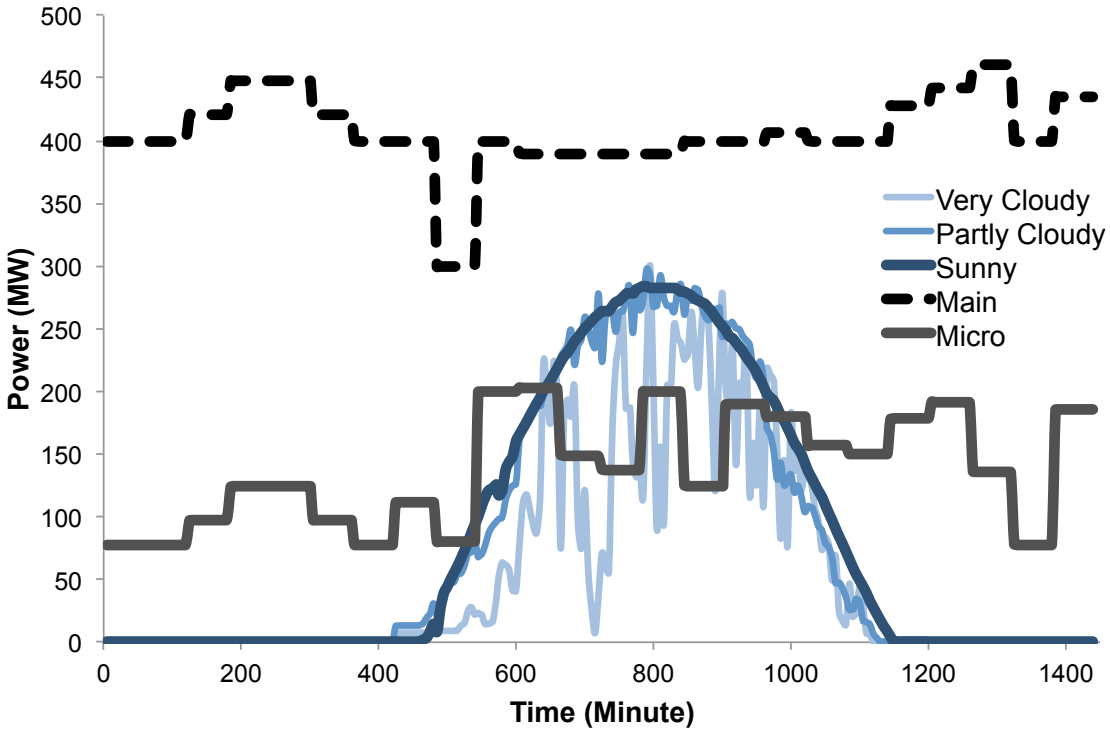

Fig. 10 Spinning and non-spinning reserve levels for the main- and microgrid juxtaposed over solar production for high, average and low scenarios

Two generators at bus 2 in the microgrid were never dispatched, and instead used for non-spinning reserve. These generators were the only two available for non-spinning reserve in stage three (the subproblem) as defined by $u_{g,t,c}^{NSP}$. This variable, indexed by scenario, allows the program flexibility to turn on or off the generator depending on if it is needed in that particular scenario. Since they were never dispatched ($u_{g,T} = 0$), it would be assumed that they would always be available ($u_{g,t,c}^{NSP} = 1$) during the subproblem. However, there were several hours where $u_{g,t,c}^{NSP} = 0$ for generator 1 or 2,

meaning the generator was not needed. It is therefore valuable to assess the generators on a per scenario basis. This information can be used to evaluate proper times to take a generator off line for maintenance.

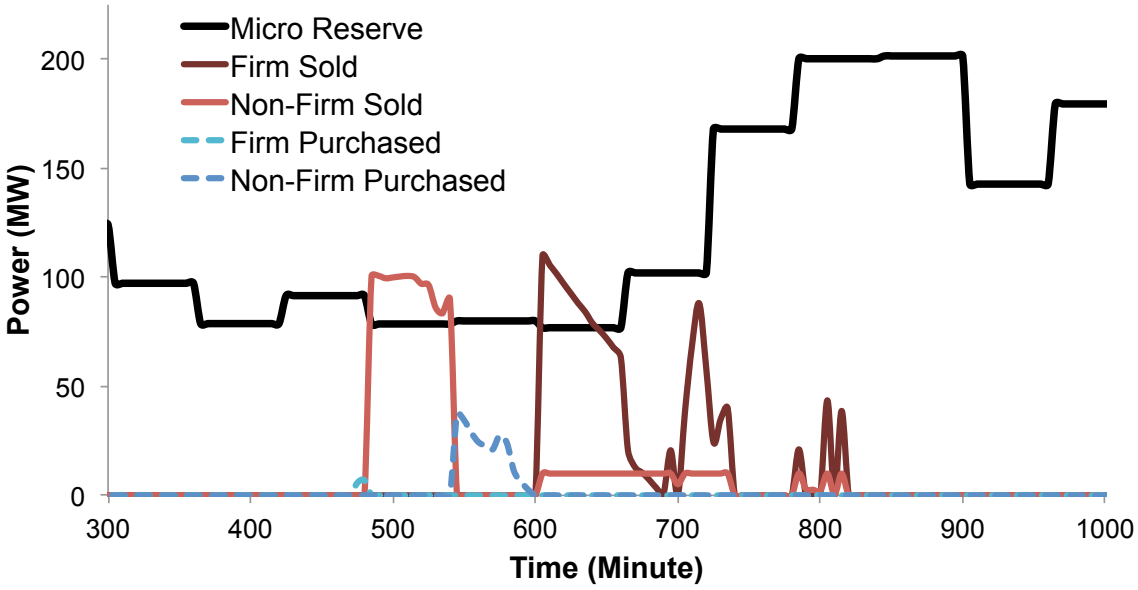

Fig. 11 Deviations in power sold and purchased are shown with the microgrid's reserve level.

In order to ensure the subproblem is feasible, load shedding and solar curtailment were allowed in stage three. There was no solar curtailment at any bus during any scenario for the solar forecasts used in this simulation. Load shedding was isolated to six instances around the 9 o'clock hour. In total, there was 0.1229 MW of load shedding in the microgrid and 0.1234 MW of load shedding the main-grid. Both values are low, and are likely to have little impact on the generator schedule. The microgrid is about a fifth the size of main-grid, making load shedding 0.024% of the microgrid demand and only 0.005% of the main-grid demand.

The main-grid's operating cost remains the same between the initial and final runs of the model as seen in Table II, which was the ensured by imposing (70). The microgrid's costs increased from the initial to the final run. Due to the added modeling

and costs associated with solar, this increase was expected. The increased cost accounts for the great deal of uncertainty in the solar forecast, which could otherwise add to costs in real-time. The additional costs add approximately 10% compared to stage one, but the total costs for the system without the additional modeling might be much greater due to the high costs to correct the dispatch in real-time. To evaluate the performance of the model, a solar scenario analysis was performed and described in the next section.

TABLE II MAIN- AND MICROGRID OPERATING COSTS

	Stage One	Final Value
Main-Grid	$448,152	$448,152
Microgrid	$250,442	$280,896

B. Solar Scenario Analysis

Similar to contingency analysis, the performance of the proposed commitment schedule is evaluated against additional solar scenarios, referred to as solar scenario analysis in this paper. The model created for the solar scenario analysis is a five-minute OPF model that allows for load shedding and solar curtailment. The reserve requirements in the model deviate slightly from the requirements in (6.23)-(6.26), since those are meant to account for solar uncertainty. The solar scenario analysis still imposes traditional reserve requirements that are necessary conditions to ensure N-1 reliability while the reserves acquired to protect against solar uncertainty are utilized. Although the hourly imports were fixed from the original model, the net power imports were allowed to vary by 2% above and below the hourly level. The deviation is intended to capture the variations that can be handled in real-time by area control error (ACE). Deviations of 2%

can likely be handled by an operator in real-time, but any variation in imports beyond this level might lead to load shedding.

The scenarios used were generated in the same method described in Chapter V-B, using Monte Carlo simulation for clear, partly cloudy, and cloudy days. Table III shows the results when analyzing the proposed schedule against 100 scenarios. The 8.64 MW of expected load shedding is roughly 1.70%, which demonstrates the ability for the stochastic programming approach to ensure a high level of reliability, especially since the subproblem had 5-minute intervals in order to capture solar uncertainty appropriately. Although load shedding was allowed for the entire system, the only load shed was in the microgrid. The percent of load shed in the microgrid is higher compared to the original model, which is to be expected. The model was optimized for the seven forecasts in stage three, whereas 100 new scenarios were used to test the validity of that model and those forecasts.

Depending on the certainty of the day-ahead solar forecast, the analysis can be adjusted to reflect different probabilities. In this case, the probability of a sunny day was 60%, partly cloudy was 30%, and very cloudy was 10%. These values can be altered on a case-by-case basis. Changing the probabilities can impact load shedding as well as curtailment. Solar curtailment was almost negligible at 0.02 MW or 0.007% of solar. Given the microgrid resources, curtailment is a lesser concern than load shedding. If the penetration of solar generation increased, curtailment might be a larger problem.

The amount of power purchased or sold in the microgrid deviated only slightly with little variability across scenarios. These deviations represent the amount of power that might need to be purchased or sold during the next day. If there is no available seller

or buyer, the microgrid can plan ensure that an emergency generator or storage device available. Continued use of the solar scenario analysis can help size emergency generation or storage for the microgrid. If import deviation levels continued to be around the same amount, a battery storage unit of that size can be purchased for use in case of contingencies and small variations in solar output. This solar scenario analysis can also help operators consider worst-case scenarios, and provide some information about periods or forecasts that produce a great deal of load shedding.

TABLE III SOLAR SCENARIO ANALYSIS RESULTS

		Load Shed (MW)	Solar Curtailed (MW)	Net Imports Sold	Net Imports Purchased
Expectation/ Period	MW	8.64	0.02	0.41	1.26
	%	1.70	$6.5*10^{-5}$	$1.5*10^{-3}$	$1.3*10^{-3}$
Standard Deviation		4.76	0.05	0.02	0.04
Maximum Value		24.17	0.28	0.46	1.35

VIII. Conclusions and Future Work

This research focuses on the issues and difficulties with modeling microgrids and solar generation in a power system. The model leverages the existing flexibility between systems and takes advantage of stochastic programming algorithms. There are several conclusions that can be drawn from the results of this work about the efficacy of modeling microgrids and solar in such great detail for a day-ahead framework.

A system with a large concentration of solar generation must plan for the variability *and* uncertainty of the resource. Past research has focused on the variability of solar by improving forecasting methodology, but rarely has addressed this issue in a day-ahead time frame. By modeling solar production on a five-minute basis, the resulting commitment schedule reflects the variability of solar output on a much more accurate time scale. While uncertainty is well studied for wind generation, solar is a unique resource with different output characteristics. The scenarios, or forecasts in this model, account for the maximum and minimum solar radiation levels as well as its distinct probability distribution.

Many have pointed to the potential reliability and controllability of microgrids in the future electric grid. In today's electric grid in the United States, trading is prevalent within different control areas. Yet, the flexibility of microgrids and opportunities for trading have not been modeled in detail for these types of systems. It is important for small systems or microgrids to draw on and account for their neighbors. If islanding is not necessary for security, then trading with the neighboring system reduces costs and improves reliability without additional capital and operational costs. Differentiating between firm and non-firm trading in day-ahead planning allows for shared reserve

requirements, which creates a more efficient dispatch solution by enabling risk to be optimally traded among neighbors. In order to utilize the resources that their grids can provide, it is important for microgrids to model their neighbors extensively while still ensuring they are not negatively impacted. Enforcing Pareto improvements for each system is crucial; otherwise, the trading of power and ancillary services might not be appealing to the main-grid. Both systems must be better off (or the same) for consistent and mutually beneficial trading. Although this model is more complex than most UC models, the microgrid is likely to see long-term benefits. Additionally, advances in stochastic programming will greatly reduce the computational burden of these complex systems.

The operating costs for the microgrid in Table II show that additional considerations made in the mathematical modeling can cost up to 10% more than a system that only accounts for simple systems interactions and a single hourly forecast. However, that additional 10% represents a small hedge against subsequent large adjustments or purchases due to solar uncertainty and leads to a negligible amount of load shedding. The load shed only reaches 1.7% when compared to 100 possible scenarios from a wide variety of possible forecasts.

This model also suggests that flexibility in planning and operations is essential. The results show that the microgrid often switched its intertie lines, signifying that leaving all lines connected was only sometimes advantageous to their system. Flexibility is also seen in the amount of deviation in the five-minute model for imports (Fig. 11). These deviations show that the microgrid might not always be able to account for extreme variations in solar output. The microgrid can preemptively change its import

level or note that actions might need to be taken in real-time. If consistent adjustments are made, the information could lead to more accurate investments in energy storage or emergency generation.

The conclusions drawn from the model can only be relevant to a limited expected forecast without validation and further simulations of the results. When compared to Monte Carlo simulations of other potential forecasts, the results show few adjustments, if any, would need to be made. The solar scenario analysis could be one way for operators to ensure that the output from the model can withstand a multitude of possible forecasts. These techniques allow a microgrid to protect itself from load shedding and create a cost effective and reliable day-ahead model to run its system.

While there are many complexities in the model, it does not account for any kind of energy storage or additional grid resources. Future work could include modeling for energy storage devices, such as large batteries. When connected near a solar panel array, these batteries could help mitigate short periods of solar variability, especially during peak times of the day. Additional modeling would be required, since constant cycling will degrade the lifetime of the battery. Other forms of storage could also be modeled; however, devices like flywheels and pumped storage are less feasible for small systems.

Electric vehicles could also act to mitigate the variability of solar by discharging their batteries while connected to a charging system. The batteries offer a very fast response time, especially when compared to traditional emergency generation. Research has been done on economic models for electric vehicle charging, an incentive that can be very appealing to a small microgrid. Electric vehicles are often plugged in during the

middle of the day, when demand is at its peak. If they were to be discharged during that time, the peak would reduce and lessen the need for additional generation.

Responsive demand is another way to alleviate the effects of solar that can be added to the day-ahead model. Certain homes or businesses in the microgrid could designate particular loads as non-essential, allowing operators to either reduce power or cut power to the load. Other approaches would allow customers to voluntarily reduce their load if they saw the cost of electricity was increasing. This might be especially useful for residential customers in a microgrid who work outside of their home during the day; seeing prices rise, a customer would be able to increase the temperature on their air conditioning unit by several degrees to decrease demand.

Additionally, a real-time model can be developed based on the day-ahead UC model. By examining the commitment schedule in a real-time framework, the results can be further assessed. Day-ahead forecasts from a local utility or operator could be obtained and tested in the UC model, and then the actual solar production could be tested with the real-time model. This would further verify the structure of the model or indicate where adjustments can be made. With advances in stochastic programming, both the day-ahead and a real-time model could be scaled for much larger systems. By using techniques that speed up convergence like progressive hedging, utilities or control areas could use this type of model on a daily basis. These models aim to help our capability to improve the management of neighboring systems and appropriately integrate renewable and variable resources.

REFERENCES

[1] J. Watson, D. L. Woodruff, and D. R. Strip, "Progressive hedging innovations for a stochastic spare parts support enterprise problem," 2007. [Online]. Available: https://cfwebprod.sandia.gov/cfdocs/CCIM/docs/phenterprise.pdf.

[2] N. V. Sahinidis, "Optimization under uncertainty: state-of-the-art and opportunities," *Computers & Chemical Engineering*, vol. 28, no. 6–7, pp. 971–983, Jun. 2004.

[3] V. Miranda and J. T. Saraiva, "Fuzzy modelling of power system optimal load flow," *IEEE Power Industry Computer Application Conf.*, pp. 386–392, 1991.

[4] B. A. Gomes and J. T. Saraiva, "Demand and generation cost uncertainty modelling in power system optimization studies," *Electric Power Systems Research*, vol. 79, no. 6, pp. 1000–1009, 2009.

[5] P. A. Pajan and V. L. Paucar, "Fuzzy power flow: considerations and application to the planning and operation of a real power system," *IEEE Power System Technology*, vol. 1. pp. 433–437 vol.1, 2002.

[6] S. Saneifard, N. R. Prasad, and H. A. Smolleck, "A fuzzy logic approach to unit commitment," *IEEE Trans. Power Syst.,* vol. 12, no. 2. pp. 988–995, 1997.

[7] S. Chakraborty, T. Senjyu, A. Yona, A. Y. Saber, and T. Funabashi, "Fuzzy unit commitment strategy integrated with solar energy system using a modified differential evolution approach," *IEEE Transmission & Distribution Conf. & Expo.: Asia and Pacific,* pp. 1–4, 2009.

[8] H. Chen, H. Li, R. Ye, and B. Luo, "Robust scheduling of power system with significant wind power penetration," in *IEEE Power and Energy Society General Meeting,* 2012, pp. 1–5.

[9] A. T. Saric and A. M. Stankovic, "Finitely adaptive linear programming in robust power system optimization," in *IEEE Power Tech,* Lausanne, 2007, pp. 1302–1307.

[10] R. Jiang, M. Zhang, G. Li, and Y. Guan, "Two-stage robust power grid optimization problem," *submitted to Journal of Operations Research*, pp. 1–34, 2010.

[11] C. Zhao, J. Wang, J.-P. Watson, and Y. Guan, "Multi-stage robust unit commitment considering wind and demand response uncertainties," *IEEE Trans. Power Syst.*, vol. PP, no. 99, pp. 1–10, 2013.

[12] D. Bertsimas, E. Litvinov, X. A. Sun, J. Zhao, and T. Zheng, "Adaptive robust optimization for the security constrained unit commitment problem," *IEEE Trans. Power Syst.*, vol. 28, no. 1, pp. 52–63, Feb. 2013.

[13] R. Jiang, J. Wang, M. Zhang, and Y. Guan, "Two-stage minimax regret robust unit commitment," *IEEE Trans. Power Syst.*, vol. PP, no. 99. pp. 1–12, 2013.

[14] C. Zhao and Y. Guan, "Unified stochastic and robust unit commitment," *IEEE Trans. Power Syst.*, vol. PP, no. 99. pp. 1–9, 2013.

[15] P. Carpentier, G. Gohen, J.-C. Culioli, and A. Renaud, "Stochastic optimization of unit commitment: a new decomposition framework," *IEEE Trans. Power Syst.*, vol. 11, no. 2, pp. 1067–1073, 1996.

[16] S. Takriti, J. R. Birge, and E. Long, "A stochastic model for the unit commitment problem," *IEEE Trans. Power Syst.*, vol. 11, no. 3. pp. 1497–1508, 1996.

[17] L. Wu, M. Shahidehpour, and T. Li, "Stochastic security-constrained unit commitment," *IEEE Trans. Power Syst.*, vol. 22, no. 2, pp. 800–811, 2007.

[18] P. A. Ruiz, C. R. Philbrick, E. Zak, K. W. Cheung, and P. W. Sauer, "Uncertainty management in the unit commitment problem," *IEEE Trans. Power Syst.*, vol. 24, no. 2, pp. 642–651, 2009.

[19] V. S. Pappala, I. Erlich, K. Rohrig, and J. Dobschinski, "A stochastic model for the optimal operation of a wind-thermal power system," *IEEE Trans. Power Syst.*, vol. 24, no. 2. pp. 940–950, 2009.

[20] A. Tuohy, S. Member, P. Meibom, E. Denny, and M. O. Malley, "Unit commitment for systems with significant wind penetration," *IEEE Trans. Power Syst.*, vol. 24, no. 2, pp. 592–601, 2009.

[21] R. Barth, H. Brand, P. Meibom, and C. Weber, "A stochastic unit-commitment model for the evaluation of the impacts of integration of large amounts of intermittent wind power," *IEEE Int. Conf. Probabilistic Methods Applied to Power Systems,* Stockholm, Sweden, pp. 1–8, 2006.

[22] F. Bouffard and F. D. Galiana, "Stochastic security for operations planning with significant wind power generation," *IEEE Trans. Power Syst.*, vol. 23, no. 2. pp. 306–316, 2008.

[23] B. C. Ummels, M. Gibescu, E. Pelgrum, W. L. Kling, and A. J. Brand, "Impacts of wind power on thermal generation unit commitment and dispatch," *IEEE Trans. Energy Convers.*, vol. 22, no. 1. pp. 44–51, 2007.

[24] J. Wang, M. Shahidehpour, and Z. Li, "Security-constrained unit commitment with volatile wind power generation," *IEEE Trans. Power Syst.* vol. 23, no. 3. pp. 1319–1327, 2008.

[25] Y. Wang, Q. Xia, and C. Kang, "A novel security stochastic unit commitment for wind-thermal system operation," in *IEEE Int. Conf. Electric Utility Deregulation and Restructuring and Power Technologies*, 2011, pp. 386–393.

[26] Q. Wang, Y. Guan, and J. Wang, "A chance-constrained two-stage stochastic program for unit commitment with uncertain wind power output," *IEEE Trans. Power Syst.*, vol. 27, no. 1. pp. 206–215, 2012.

[27] M. Rothleder, U. Helman, C. Loutan, and S. Venkataraman, "Integration of wind and solar under a 20% RPS: stochastic simulation methods and results from California ISO studies," in *IEEE Power and Energy Society General Meeting*, 2012, pp. 1–8.

[28] California ISO, "Integration of renewable resources: technical appendices for California ISO renewable integration studies," Caliornia ISO, Folsom, CA, 2010. [Online]. Available: http://www.caiso.com/282d/282d85c9391b0.pdf.

[29] A. Y. Saber and G. K. Venayagamoorthy, "Resource scheduling under uncertainty in a smart grid with renewables and plug-in vehicles," *IEEE Syst. J.*, vol. 6, no. 1, pp. 103–109, 2012.

[30] M. Castro, J. Peire, J. Carpio, M. Valcarcel, and F. Aldana, "Large grid solar energy integration analysis," *Conf. Industrial Electronics Society*, vol. 3. pp. 575–580, 1988.

[31] R. Huang, T. Huang, R. Gadh, and N. Li, "Solar generation prediction using the ARMA model in a laboratory-level micro-grid," *IEEE Int. Conf. Smart Grid Communications*, pp. 528–533, 2012.

[32] M. Rizwan, M. Jamil, and D. P. Kothari, "Generalized neural network approach for global solar energy estimation in india," *IEEE Trans. Sustain. Energy*, vol. 3, no. 3. pp. 576–584, 2012.

[33] L. P. Naing and D. Srinivasan, "Estimation of solar power generating capacity," in *IEEE Int. Conf. Probabilistic Methods Applied to Power Systems*, 2010, pp. 95–100.

[34] C. Tao, D. Shanxu, and C. Changsong, "Forecasting power output for grid-connected photovoltaic power system without using solar radiation measurement," in *IEEE Int. Symp. Power Electronics for Distributed Generation Systems*, 2010, pp. 773–777.

[35] T. Senjyu, S. Chakraborty, A. Y. Saber, H. Toyama, A. Yona, and T. Funabashi, "Thermal unit commitment strategy with solar and wind energy systems using genetic algorithm operated particle swarm optimization," *IEEE Power and Energy Conf.,* pp. 866–871, 2008.

[36] M. J. R. Perez and V. Fthenakis, "Impacts of long-timescale variability in solar resources at high pv penetrations: quantification," in *IEEE Photovoltaic Specialists Conf.*, 2012, pp. 2481–2486.

[37] Y. V Makarov, S. Lu, N. Samaan, Z. Huang, K. Subbarao, P. V Etingov, J. Ma, R. P. Hafen, R. Diao, and N. Lu, "Integration of uncertainty information into power system operations," in *IEEE Power and Energy Society General Meeting*, 2011, pp. 1–13.

[38] A. P. S. Meliopoulos, "Challenges in simulation and design of μgrids," *IEEE Power Engineering Society Winter Meeting*, vol. 1. pp. 309–314 vol.1, 2002.

[39] H. Jiayi, J. Chuanwen, and X. Rong, "A review on distributed energy resources and microgrid," *Renewable and Sustainable Energy Reviews*, vol. 12, no. 9, pp. 2472–2483, Dec. 2008.

[40] C. Marnay, F. J. Robio, and A. S. Siddiqui, "Shape of the microgrid," *IEEE Power Engineering Society Winter Meeting*, vol. 1, pp. 150–153, 2001.

[41] C. Marnay and G. Venkataramanan, "Microgrids in the evolving electricity generation and delivery infrastructure," in *IEEE Power Engineering Society General Meeting*, 2006, p. 5 pp.

[42] R. H. Lasseter and P. Paigi, "Microgrid: a conceptual solution," *IEEE Power Electronics Specialists Conf.*, vol. 6, pp. 4285–4290, 2004.

[43] P. Siano, C. Cecati, H. Yu, and J. Kolbusz, "Real time operation of smart grids via fcn networks and optimal power flow," *IEEE Trans. Ind. Informat.*, vol. 8, no. 4, pp. 944–952, 2012.

[44] S.-J. Ahn, S.-R. Nam, J.-H. Choi, and S.-I. Moon, "Power scheduling of distributed generators for economic and stable operation of a microgrid," *IEEE Trans. Smart Grid*, vol. 4, no. 1, pp. 398–405, 2013.

[45] R. Lasseter and P. Piagi, "Control and design of microgrid components," PSERC, Madison, WI, Pub. 06-03, 2006.

[46] H. Kanchev, B. Francois, and V. Lazarov, "Unit commitment by dynamic programming for microgrid operational planning optimization and emission

reduction," *IEEE Int. Electrical Machines and Power Electronics and Electromotion Joint Conf.*, pp. 502–507, 2011.

[47] H. Kanchev, V. Lazarov, and B. Francois, "Environmental and economical optimization of microgrid long term operational planning including PV-based active generators," *IEEE Int. Power Electronics and Motion Control Conf.*, pp. LS4b–2.1–1–LS4b–2.1–8, 2012.

[48] A. M. Zein Alabedin, E. F. El-Saadany, and M. M. A. Salama, "Generation scheduling in microgrids under uncertainties in power generation," *IEEE Electrical Power and Energy Conf.*, pp. 133–138, 2012.

[49] H. Z. Liang and H. B. Gooi, "Unit commitment in microgrids by improved genetic algorithm," *Conf. Proc. IPEC,* pp. 842–847, 2010.

[50] X. Wu, X. Wang, and Z. Bie, "Optimal generation scheduling of a microgrid," *IEEE Int. Conf. and Expo. Innovative Smart Grid Technologies*, pp. 1–7, 2012.

[51] M. E. Khodayar, M. Barati, and M. Shahidehpour, "Integration of high reliability distribution system in microgrid operation," *IEEE Trans. Smart Grid*, vol. 3, no. 4, pp. 1997–2006, 2012.

[52] R. Palma-Behnke, C. Benavides, F. Lanas, B. Severino, L. Reyes, J. Llanos, and D. Saez, "A microgrid energy management system based on the rolling horizon strategy," *IEEE Trans. Smart Grid*, vol. 4, no. 2. pp. 996–1006, 2013.

[53] M. Salani, A. Giusti, G. Di Caro, A.-E. Rizzoli, and L. M. Gambardella, "Lexicographic multi-objective optimization for the unit commitment problem and economic dispatch in a microgrid," *IEEE Int. Conf. and Expo. Innovative Smart Grid Technologies,* pp. 1–8, 2011.

[54] A. J. Wood and B. F. Wollenberg, *Power Generation Operation and Control*, 2nd ed. New York: John Wiley & Sons, Inc., 1996.

[55] A. Castillo and R. P. O'Neill, "Optimal power flow paper 4: survey of approaches to solving the ACOPF," FERC, Washington D.C., 2013.

[56] M. B. Cain, R. P. O'Neill, and A. Castillo, "Optimal power flow paper 1: history of optimal power flow and formulations," FERC, Washington D.C., 2012.

[57] R. P. O'Neill, A. Castillo, and M. B. Cain, "Optimal power flow paper 2: the IV formulation and linear approximations of the ac optimal power flow problem," FERC, Washington D.C., 2012.

[58] R. P. O'Neill, A. Castillo, and M. B. Cain, "Optimal power flow paper 3: the computational testing of ac optimal power flow using the current voltage formulations," FERC, Washington D.C., 2012.

[59] K. W. Hedman, R. P. O'Neill, and S. S. Oren, "Analyzing valid inequalities of the generation unit commitment problem," in *IEEE Power Systems Conf. and Expo.*, 2009, pp. 1–6.

[60] K. W. Hedman, "Flexible transmission in the smart grid," Ph.D. dissertation, Dept. Ind. Eng. and Operations Research, Univ. California, Berkeley, 2010.

[61] G. B. Sheble and G. N. Fahd, "Unit commitment literature synopsis," *IEEE Trans. on Power Syst.*, vol. 9, no. 1, pp. 128–135, 1994.

[62] N. P. Padhy, "Unit commitment-a bibliographical survey," *IEEE Trans. on Power Syst.*, vol. 19, no. 2, pp. 1196–1205, 2004.

[63] H. Y. Yamin, "Review on methods of generation scheduling in electric power systems," *Electric Power Systems Research*, vol. 69, no. 2–3, pp. 227–248, May 2004.

[64] J. Tang, D. Wang, R. Y. K. Fung, and K.-L. Yung, "Understanding of fuzzy optimization: theories and methods," *J. Syst. Sci. and Complexity*, vol. 17, no. 1, 2004.

[65] NREL, "University of Texas at El Paso solar radiation data," *NREL Cooperative Networks For Renewable Resourece Measurements*, 1997. [Online]. Available: rredc.nrel.gov/solar/new_data/confrrm/ep/.

[66] J. Ma, Y. V Makarov, C. Loutan, and Z. Xie, "Impact of wind and solar generation on the California ISO's intra-hour balancing needs," in *IEEE Power & Energy Society General Meeting*, 2011, no. 1, pp. 1–6.

[67] California ISO, "Integration of renewable resources: operational requirements and generation fleet capability at 20% RPS," California ISO, Folsom, CA, 2010.

[68] B. Luong, "Truncated gaussian," *Matlab Central*, 2009. [Online]. Available: http://www.mathworks.com/matlabcentral/fileexchange/23832-truncated-gaussian.

[69] J. F. Benders, "Partitioning procedures for solving mixed-variables programming problems," *Numerische Mathematik*, vol. 4, no. 1, pp. 238–252, 1962.

[70] G. L. Nemhauser and L. A. Wolsey, *Integer and Cominbatorial Optimization*. New York: A Wiley-Interscience Publication John Wiley & Sons, Inc., 1999.

[71] H. Ma, S. M. Shahidehpour, and M. K. C. Marwali, “Transmission constrained unit commitment based on benders decomposition,” *Proc. American Control Conf.*, vol. 4, pp. 2263–2267, 1997.

[72] S. J. Kazempour, S. Member, and A. J. Conejo, “Strategic generation investment under uncertainty via Benders decomposition,” *IEEE Trans. Power Syst.*, vol. 27, no. 1, pp. 424–432, 2012.

[73] N. Laothumyingyong and P. Damrongkulkamjorn, “Security-constrained unit commitment using mixed-integer programming with Benders decomposition,” in *Int. Conf. Electrical Engineering/Electronics Computer Telecommunications and Information Technology*, 2010, pp. 626–630.

[74] Y. Li and J. D. McCalley, “A general Benders decomposition structure for power system decision problems,” *Int. Conf. Electro/Information Technology,* pp. 72–77, 2008.

[75] E. B. Fisher, R. P. O’Neill, and M. C. Ferris, “Optimal transmission switching,” *IEEE Trans. Power Syst.*, vol. 23, no. 3, pp. 1346–1355, 2008.

[76] K. W. Hedman, M. C. Ferris, R. P. O’Neill, E. B. Fisher, and S. S. Oren, “Co-optimization of generation unit commitment and transmission switching with N-1 reliability,” *IEEE Trans. Power Syst.*, vol. 25, no. 2, pp. 1052–1063, 2010.

[77] C. Grigg, “Power systems test case archive: reliability test system (RTS) - 1996,” 1996. [Online]. Available: http://www.ee.washington.edu/research/pstca/rts/pg_tcarts.htm.

[78] C. Grigg, P. Wong, P. Albrecht, R. Allan, M. Bhavaraju, R. Billinton, Q. Chen, C. Fong, S. Haddad, S. Kuruganty, W. Li, R. Mukerji, D. Patton, N. Rau, D. Reppen, A. Schneider, M. Shahidehpour, and C. Singh, “The IEEE reliability test system-1996. a report prepared by the reliability test system task force of the application of probability methods subcommittee,” *IEEE Trans. Power Syst.*, vol. 14, no. 3, pp. 1010–1020, 1999.